Wireless surface stimulator

Gergely Andor Maksay

August 21, 2009

Matriculation number: 0803879

Academic year 2008/2009

first supervisor: Dr. Bernd Porr

second supervisor: Dr. Khaled Elgaid

Abstract

Functional electrical stimulation (FES) is the stimulation of peripheral nerves on innervated paralysed muscle groups with the purpose of facilitating a functional movement. It is excercised in particularly to aid the rehabilitation of people with paraplegia. For that application, a low cost, portable, battery powered neuromuscular surface stimulation system was developed and implemented, which is capable of delivering high voltage, constant current controlled faradic pulse trains through surface electrodes. The stimulation waveform is flexibly adjustable by the current amplitude (0-100 mA), the pulse width (40-500 μs), and the repetition frequency of pulses (25-300 Hz). These parameters can be remotely configured from a personal computer over a wireless sub 1 GHz radio frequency link. The entire system consists of the stimulator board, an interface board responsible for the wireless transmission of commands from the PC, and the Matlab software which interacts with the operator through a graphical user interface. The stimulator is microcontroller based and the output stage consists of a minimalistic modified boost converter. Special efforts were made to optimise the device for low power consumption. Besides it's intended application field the system is apt to be universally used for therapy and research.

Contents

1 Introduction **1**

2 Neuromuscular stimulation **2**
2.1 Nerve and muscle cells 2
2.2 Electrical stimulation in practice 2
2.3 Functional electrical stimulation (FES) 4
2.4 Impedance model of skin 5

3 Stimulator output stage **7**
3.1 Boost regulators 7
3.2 Output stage 9
3.3 Selection of circuit components 17
3.4 Current consumption 18
3.5 Closed loop control 18

4 Wireless communication **20**
4.1 CC1000 20
4.2 Antenna design 24

5 Overall system description **26**
5.1 Wireless stimulator 26
5.1.1 Hardware description 26
5.1.2 Software description 28
5.2 RS232/Wireless interface 36
5.2.1 Hardware description 36
5.2.2 Software description 37

6 Performance analysis **41**

7 User's guide **46**

8 Future development plans **49**

9 Conclusion **51**

List of Figures

1 Waveform of biphasic pulses and nomenclature of pulse properties 4
2 Equivalent electrical model of electrodes, skin and tissue 6
3 Boost regulator 7
4 Boost regulator, while transistor is on 8
5 Boost regulator, while transistor is off 8
6 Stimulator output stage 9
7 Inductor current and voltage in a boost regulator (no load) . . 12
8 Spice simulations of rising output voltage, if boost converter's load is removed 14
9 Spice simulation of output stage 16
10 Block diagram explaining the closed loop control of the boost converter 19
11 The complete output stage of the stimulator 19
12 Block diagram of the CC1000 [21], with permission of TI 22
13 Transmitted power spectrum of the FSK modulated system, rough estimation 23
14 Synchronous Manchester encoding [21], with permission of TI . . 24
15 The wireless stimulation system 26
16 Block diagram of wireless stimulator 27
17 Functional block diagram of the MSP430F2122 microcontroller[17], with permission of TI 27
18 Main() function of wireless stimulation software 30
19 PWM generation of Timer_A1 and Timer_A2 31
20 Algorithm for implementing the digital controller 33
21 Flowchart of the wireless communication handling 35
22 Block diagram of RS232/Wireless interfacing board 36
23 Flowchart for Main() function of Interfacing board 37
24 Flowchart of external interrupt handling in the main loop 38
25 Timer_A0 ISR for button polling 39
26 The USCI interrupt routine in main loop 40
27 Oscilloscope measurements of stimulator output pulses 44
28 Front view image of the boards 46
29 Matlab program's graphical user interface 47

List of Tables

1 Technical details of RehaStim stimulator 1
2 Typical current consumption of the CC1000 [21] 20
3 Packet format 34
4 Data Field of 'Update' packets 34
5 Source files of the software 36
7 Estimated power consumption of the stimulator 42
8 Characteristics of the wireless stimulator in comparison with the specified technical details of RehaStim[2]. 43

List of Abbreviations

AC	Alternating current
ADC	Analog-digital converter
BER	Bit error rate
BJT	Bipolar junction transistor
CMOS	Complementary metal–oxide–semiconductor
CPU	Central processing unit
DC	Direct current
DCO	Digitally Controlled Oscillator
EEG	Electroencephalogram
EMG	Electromyogram
ENG	Electroneurogram
FES	Functional electrical stimulation
FET	Flash emulation tool
FSK	Frequency shift keying
GCC	GNU compiler collection
GDB	GNU debugger
GPIO	General purpose input/output
GUI	Graphical user interface
IC	Integrated circuit
IF	Intermediate frequency
ISM	Industrial, Scientific and Medical
ISR	Interrupt service routine
ITU	International Telecommunication Union
JTAG	Joint Test Action Group
LED	Light emitting diode
LNA	Low noise amplifier
LPF	Low pass filter
MCU	Microcontroller unit
MOSFET	Metal–oxide–semiconductor Field-effect transistor
NRZ	Non return to zero
PA	Power amplifier
PC	Personal computer
PCB	Printed circuit board
PD	Phase detector
PD	Power down mode
PLL	Phase locked loop
PWM	Pulse width modulation
RAM	Random access memory
RISC	Reduced instruction set computing

SMPS	Switched mode power supply
TACCR	Timer_A capture/compare register
TAR	Timer_A register
TI	Texas Instruments
TSSOP	Thin-shrink Small Outline Package
UART	Universal asynchronous receiver/transmitter
UHF	Ultra high frequency
USB	Universal serial bus
USCI	Universal serial communication interface
VCO	Voltage controlled oscillator

1 Introduction

The Centre for Rehabilitation Engineering at the University of Glasgow has been actively engaged in research on functional electrical stimulation (FES) with cycling for the rehabilitation of people with paraplegia. In cooperation with Hasomed GmbH, they developed a FES tricycle system, named RehaBike, which is based on the neuromuscular stimulator of Hasomed, called RehaStim. This paper aims to describe a stimulator device which I designed and built as a low cost alternative to RehaStim, but contrary to RehaStim it is lightweight, portable, battery powered, and, most importantly, it is capable to be controlled over a wireless link from a laptop or personal computer (PC). In addition, I put enormous effort to minimising the power consumption of the stimulator as much as possible, and reduce its size, so patients will be able to directly mount the stimulator board to the intended application surface on their body.

Like RehaStim, the designed stimulator is meant to perform neuromuscular surface stimulation of the various muscles in the lower extremities, which are involved in cycling movement. The stimulation output is a series of constant current regulated pulses, whose parameters are flexibly adjustable. It was my intention to investigate how close the performance of a professional stimulator module can be approached with a simple, low cost design. Therefore, I aimed to achieve the specified technical details of RehaStim, shown in Table 1.

	minimum	maximum
current	0	126 mA
pulse width	$20\mu s$	500 μs
frequency	1 Hz	140 Hz
pulse form	any	
number of channels	8	

Table 1: Technical details of RehaStim stimulator

Wireless interfacing with a PC was also implemented, and a user-friendly graphical user interface was created for the configuration of the basic stimulation parameters.

Section 2 will give an introduction to electrical muscle stimulation and the underlying biological basis, with special emphasis on functional electrical stimulation. Sections 3 and 4 will describe the two most challenging design tasks in this project, the high voltage generation and the wireless communication. Section 5 will provide the detailed hardware and software description of my design, and Section 6 will analyse its achieved performance. Section 7 is a User's Guide of the complete stimulation system, with detailed description how the device should be operated.

2 Neuromuscular stimulation

A long time elapsed since Luigi Galvani first discovered that frog muscles twitch by the application of electrical current. Today, electrotherapy became a standard practice in medicine. It is used to cure neurological diseases, facilitate wound ailment, recover muscle functions after spinal cord injury, just to name a few. This section will discuss the basic concepts of electrical stimulation with a brief introduction to the biology of nerve and muscle cells, which is utterly necessary to understand the further discussion in this section. After then, functional electrical stimulation, the intended application field of the subject device will be introduced, and the most important specifications of a common stimulator will be examined. Most of the presented information was gathered from [3, 4, 5], unless otherwise noted.

2.1 Nerve and muscle cells

Cells contain lower concentration of positive cations, than the surrounding extracellular fluid, which causes a potential difference between the two sides of the cell membrane. The electronegative voltage of cells is called resting potential, and it is sustained by active biochemical and electrostatical processes. It is possible to reverse this voltage in nerve cells (neurons) and muscle cells (muscle fibres) by depolarising the cell membrane with sufficiently intense electric field (current) of sufficient duration. The excitation of the cell membrane produces an action potential which propagates along the lengthy nerve fibre (the axon) to the subsequent nerve or muscle cell. The links between muscle fibres and neurons are called motor units, which consist of the neurons attached to several parallel muscle fibres. An action potential on a motor unit causes a twitch on all corresponding muscle fibres. There are many motor units in a muscle. They activate with a relative phase shift and the resulting firing pattern determines the smooth muscular movement[3, 4].

2.2 Electrical stimulation in practice

The above described physiological process is natural, but the same effect can be triggered artificially by applying an electrical pulse train through the tissue. The induced current causes electric field along its path, which depolarises the membrane of motor units. The result is a twitch of the muscle. The stimulation of innervated tissue is called neuromuscular stimulation, which will be the intended application of the device presented in this document. It is also possible to stimulate denervated muscles directly, although the threshold charge for activating muscle fibres is significantly larger than that of neurons, thus opinions vary about its effectiveness. This stimulation technique is called electrical muscular stimulation.

There are various ways how stimulation electrodes can be applied. The simplest and cheapest method is to place surface electrodes on the skin noninvasively. This technique, called transcutaneous stimulation, has the disadvantage,

that the skin-electrode interface significantly heightens the impedance of the total system to be stimulated. Furthermore, a trained therapist is needed to accurately apply the electrode to the intended area. In order to achieve maximal contraction force, one electrode (called active electrode, typically the anode) must be placed over the motor points, where the largest concentration of motor units is situated. The other electrode (return electrode) is typically placed on the muscle belly[3]. Transcutaneuos stimulation might also be hurtful for patients as pain receptors are also stimulated. Alternative to surface electrodes are the invasive percutaneous and implanted electrodes, about which please refer to [5].

There are many aspects of characterising neuromuscular stimulators. They can be portable or line powered, high voltage or low voltage, their output can be constant voltage or constant current regulated, but maybe their most important feature is the waveform they produce.

There is still active research to find the optimal waveform of the applied current.

In order to stimulate denervated muscle, usually long (100 ms) *galvanic* (interrupted) DC pulses are used.

Other applications use high frequency *interferential* or *tone burst* AC pulses.

Neuromuscular stimulation, and in particular functional electrical stimulation, rather uses a low frequency ($<$100 Hz) *faradic* pulse train, which can be characterised with the amplitude of pulses, the repetition frequency of pulses and the pulse duration[3]. Because the electrode-tissue interface has capacitive properties, every delivered pulse builds up charge in the tissue which can be potentially harmful, especially in case of implanted electrodes. To prevent this, sometimes another pulse with opposite polarity (called reverse pulse) is induced to balance the net charge. This type of stimulation is called biphasic, while an unipolar pulse train is referred to as monophasic. Biphasic stimulation is generally safer, but the threshold current for activating muscle movement will be higher, as the induced electric field will be more localised. The solution is the application of pseudomorphic biphasic pulses, which are prolonged and have lower amplitudes, but still deliver the same amount of charge[6]. Figure 1 displays a biphasic pulse with the definition of the pulse parameter terminology that will be used in the rest of this paper.

The strength of muscle contraction can be controlled by the parameters of stimulation[5].

The current amplitude and pulse duration controls the total amount of injected charge. Increasing either of these parameters will result in larger electric field, more and more motoneurons (motor units) will be affected, increasing number of muscle fibres twitch which contributes to the total force of the contraction (this effect is know as spatial summation).

If the time interval of the applied stimuli is shorter than the duration of the twitch, then the exerted tension will rise additively, until the upper limit (tetanus) of contraction is reached (cumulative effect of stimulus repetition is known as temporal summation). For this reason, the stimulation frequency must be higher than the so called fusion frequency for a smooth contraction,

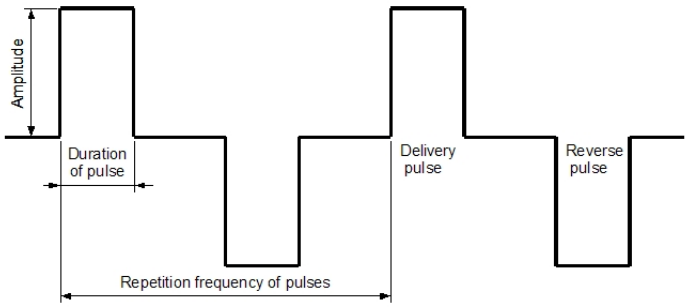

Figure 1: Waveform of biphasic pulses and nomenclature of pulse properties Note that pulse widths are unrealistically exaggerated for better demonstration reasons

otherwise the response will be a series of twitches[4]. It must be noted, that increasing stimulation frequency also increases the rate of muscle fatigue. For these reasons, the repetition frequency of pulses is usually higher than 12 Hz, but rarely exceeds 100 Hz[5].

Muscles come in different size and shape, which also determines the maximal force, susceptibility to fatigue, and the time for a twitch. Thus the parameters of stimulation must be adapted to muscle type. According to today's suggested practice slow muscles are trained with weaker, but sustained *tonic* activation, and fast muscles are rather trained with shorter, but more intense *phasic* stimuli[3].

2.3 Functional electrical stimulation (FES)

Functional electrical stimulation is the stimulation of the peripheral nerves with the purpose of facilitating some kind of functional movement. It must be distinguished from therapeutic electrical stimulation, which aims to improve tissue health and permanently restore sensory functions, and the stimulation is not necessarily accompanied by actual movement[3, 5]. It was already mentioned, that neuromuscular stimulation is only used to stimulate innervated healthy muscles. Because of this, most of the patients benefitting from this technology typically suffered spinal cord or head injury, stroke, cerebral palsy, or multiple sclerosis.

Every movement involves the contraction of a variety of muscles, and each muscle moves as the result of a very complex firing pattern of motor units. There is still significant ongoing research toward the artificial imitation of natural muscle movement. Neuroprostheses[1] have been successfully tested for the upper and lower extremities, the bowels, and the respiratory system, but even

[1] FES devices used for substituting a neurological function[5]

bladder control of patients could be recovered with FES. Several systems underwent clinical trials and are now available as commercial products. Today the main concentration area of research is the closed loop control of stimulation with feedback from a combination of biopotentials, including nerves (ENG, electroneurogram), muscles (EMG), and the brain(EEG). Others are applying implanted stimulators powered and controlled by inductive links, and connecting neuroprostheses in a network[5].

FES cycling

The Centre for Rehabilitation Engineering at the University of Glasgow and Hasomed GmbH. developed a tricycle system allowing cycling exercise with functional electrical stimulation of the leg muscles for people with paraplegia. Daily physical excercise in form of cycling can offer numerous benefits, including improved cardiorespiratory health, boosted metabolism, better endurance, recovery from muscle atrhophy and other secondary problems associated with the lack of movement, improved endurance, and general wellbeing. RehaBike is based on a stimulator device called RehaStim, which performs controlled stimulation of the paralysed leg muscles based on the position of the pedals. This project investigates a possible portable, wireless stimulator solution in conjunction with this FES cycling project[2, 1].

2.4 Impedance model of skin

In order to have accurate control over the injected charge and the resulting muscle response, current regulated stimulation must be applied. This requires basic knowledge about the electrical characteristics of the electrodes, the human skin and tissue.

The total impedance that can be measured between the electrodes depends on a variety of factors, such as current density, repetitive pulse frequency, electrode size, electrode separation, electrode material, temperature, humidity, and duration of stimulation[8]. There has been enormous research to find the best fitting equivalent circuit model, but there is still no accordance how to model its nonlinear behaviour accurately. One of the most common models is presented in Figure 2[9]. It reflects that during neuromuscular stimulation three subsystems are connected serially.

- The boundary of electrodes and skin is of special importance, because that is where the flow of electrons from the stimulator is transducted into ion flow in the tissue (which can be regarded as electrolyte as charges are carried by ions). At the boundary of every metal-electrolyte interface there is a potential difference which is called the half cell potential. The model also contains a series RC suggested by Warburg, and the faradic leakage resistance R_f accounting for DC characteristics of the model [10] .

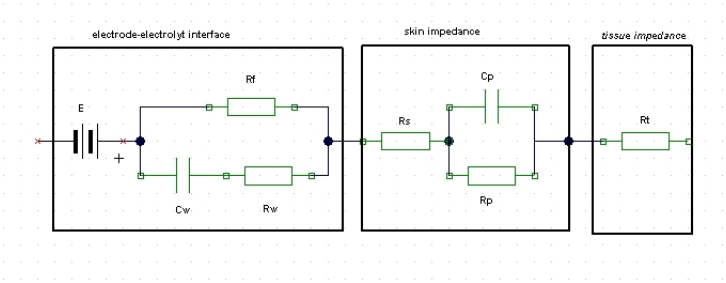

Figure 2: Equivalent electrical model of electrodes, skin and tissue

- The skin can be modeled by a serial resistance and a parallel RC. C_p and R_p can be practically eliminated by removing the outermost layer of the skin, the stratum corneum [7].
- The deep tissue can be modeled by the resistive R_t, bulk tissue resistance.

Because of the complexity of the model and the lots of contributing nonlinear physical factors it is very difficult to estimate the total impedance between the two electrodes, but [11] suggests that for practical FES applications the impedance should be in the magnitude of 1 kOhm. However if the skin is not prepared (abrasion of stratum corneum, etc.), the total impedance can be several times higher.

3 Stimulator output stage

In the earlier discussion it became apparent, that the low voltage of abattery cell will be insufficient to generate milliamp magnitude current pulses over the high resistance skin and tissue. Some sort of electrical power supply is needed for voltage multiplication, which is inexpensive, small, and has relatively high efficiency so little energy from the battery is wasted during the conversion. Switched Mode Power Supplies (SMPS) satisfy these requirements[12].

3.1 Boost regulators

The following discussion is based on [13] and [12] and assumes ideal circuit elements.

SMPSs, which convert DC voltage to DC voltage are classified as DC-DC converters. One of the simplest DC-DC converter which can output higher voltage than its input is called boost regulator (also known as boost converter). Its schematic can be seen in Figure 3.

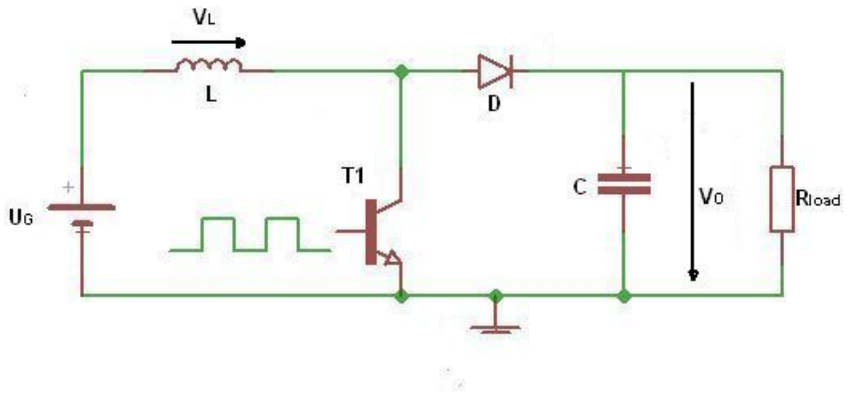

Figure 3: Boost regulator

In this circuit transistor T is operated as a switch, it is turned on and off at high frequency.

When the transistor is on, D doesn't conduct current and thus separates the RC network from the inductor (Figure 4). The energy of the inductor builds up as increasing current flows through it. At the same time, the capacitor discharges through R_{load} .

If we assume that the switching frequency is high enough and the capacitor has large capacitance, $V_o$will be almost constant (small ripple approximation):

$$V_L = V_G \tag{1}$$

$$i_C = -\frac{V_o}{R_{load}} \tag{2}$$

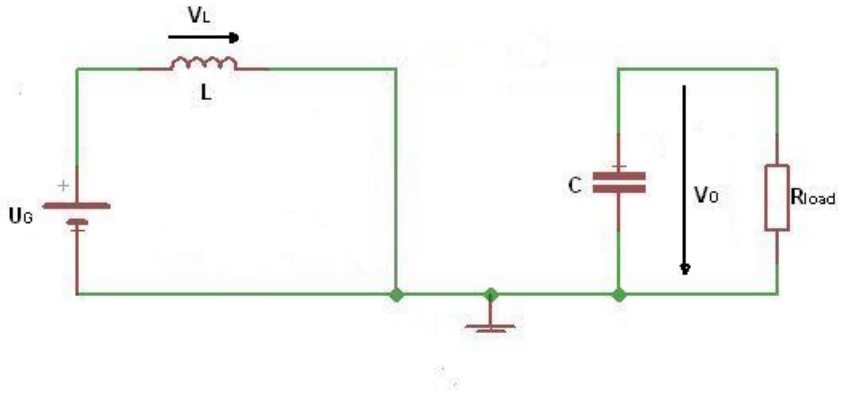

Figure 4: Boost regulator, while transistor is on

When we turn off the transistor, the magnetic energy of the inductor will be transferred to the RC network of the capacitor and the load (Figure 5). With the previous assumptions regarding voltage ripple:

$$V_L = V_G - V_o \tag{3}$$

$$i_C = I - \frac{V}{R_{load}} \tag{4}$$

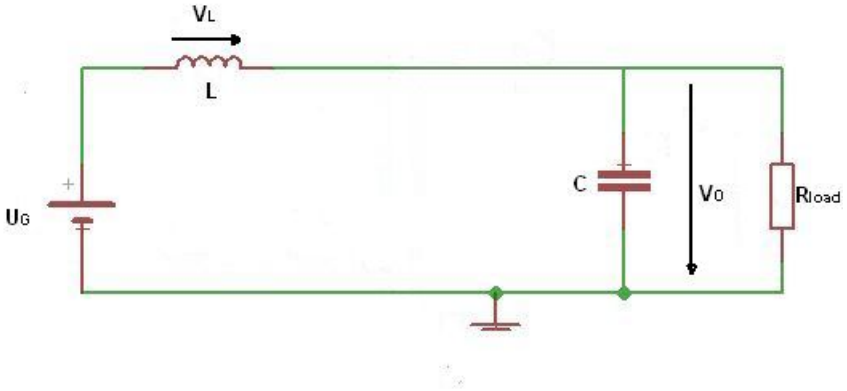

Figure 5: Boost regulator, while transistor is off

According to the principle of Volt-second balance [13]

$$V_G D T_S + (V_G - V_o)(1 - D) T_S = 0 \tag{5}$$

Where

D is the duty cycle $D = \frac{T_{ON}}{T_S}$,$0 \leq D \leq 1$,
T_{ON} is the duration while T was on,
and T_S is the switching period.
If we solve equation 5 we can calculate the DC gain:

$$\frac{V_O}{V_G} = \frac{1}{1-D} \tag{6}$$

This equation states that the output voltage of a boost converter cannot be smaller than its input voltage.

Equation 6 is only true, if the current in the inductor never falls to zero during the entire switching cycle. If this condition is met the circuit is said to be in continuous mode of operation. Otherwise, the circuit will enter discontinuous mode and the equations describing its behaviour will be more complex. Their derivation can be found in [13] and [12].

3.2 Output stage

In the muscle stimulator device a boost converter will be used to generate the needed voltage levels for a prescribed current amplitude. It is a simple and effective solution, and it was used in commercial stimulators available off the shelf.

Let's substitute R_{load} in Figure 3 by the skin and tissue resistance of the patient under therapy. This setup would supply constant current through the skin, and considering the high skin and tissue impedance discussedin section 2.4, almost unity duty cycle would be needed for current levels in the magnitude of milliamps. Practically this is unattainable, as the non zero inductor resistance drastically decreases the d.c. gain if $D \approx 1$[12].

Instead of this, R_{load} will be substituted according to Figure 6.

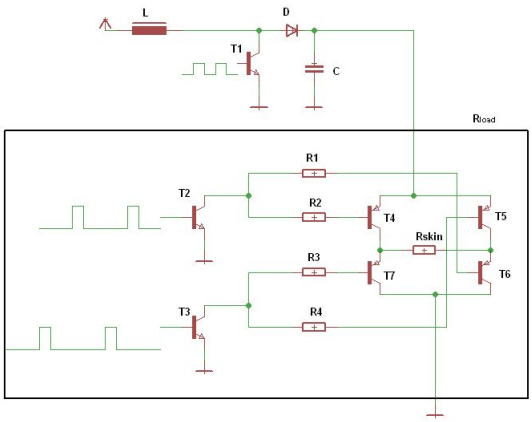

Figure 6: Stimulator output stage

With the newly introduced components it is possible to deliver current pulses for the patient, who is symbolised in the schematic by R_{skin}.

Switching on transistor T2 opens transistor T4 and T6. If we keep transistor T3 closed, current from the boost converter will flow through T4, R_{skin}, and T6 to ground. Opening T3, on the other hand, determines a current path through T5 and T7 (provided T2 is closed), which delivers current to the patient with opposite polarity. This setup enables the stimulator to transfer monophasic or biphasic current pulses, according to how transistors T2 and T3 are driven. It is very important not to open T2 and T3 at the same time, as this would cause a short circuit at the output of the boost regulator, which could ultimately destroy the device. Microcontroller software guarantees that this condition can never happen.

From the boost converter's point of view it is indifferent what the path of current is, as long as it flows through R_{skin}. This, however, will not be the case during most of the time. If both T2 and T3 are closed (no pulses are currently delivered), R_{load} will be high impedance, through which the capacitor of the SMPS cannot discharge at all. This prevents steady state operation, the output voltage will rise after each switching cycle and the equations of continuous mode (Equation 6) or discontinuous mode in [13] and [12] will fail. No other literature was found to discuss the above described condition, the following analysis is my own work, although the inital equations were based on the description of dicontinuous mode of operation in [13].

The following discussion presumes that the switching frequency (f_s) of the SMPS is much higher than the frequency of pulse repetition(f_{pulse}), and the time interval between pulses(t_{pulse}) is much longer than the pulse duration (T_p):

$$f_s = \frac{1}{T_s} >> f_{pulse} \tag{7}$$

$$t_{pulse} = \frac{1}{f_{pulse}} >> T_p \tag{8}$$

First, let's observe the behaviour of the boost regulator in Figure 3 with no load ($R_{load} = \infty$). This condition can be described by a transient discontinuous mode of operation (the inductor current falls to zero in each switching period).

When the transistor T1 is turned on, (Figure 4, $R_{load} = \infty$)

$$V_L = V_G \tag{9}$$

$$i_C = 0 \tag{10}$$

The differential equation describing the relationship between inductor current and voltage states:

$$V_L = L\frac{dI_L}{dt} \tag{11}$$

Integration over time and equation 9 shows, that while T1 is on, current in the inductor increases linearly [13]:

$$I_L = I_o + \frac{1}{L}\int V_L dt = \frac{V_G t}{L} \tag{12}$$

where I_o is the current flowing in the inductor at the beginning of the switching cycle.

Because of the transient discontinuous mode of operation $I_o = 0$, the inductor transfers all of its energy to the capacitor in each cycle. As soon as $I_L$drops to 0, D diode becomes reverse biased and stops conducting which avoids any further decline of I_o (see Figure 7).

The maximal current in the inductor is

$$I_{L,max} = \frac{V_G T_{on}}{L} \tag{13}$$

where

$$T_{on} = DT = \frac{D}{f_s} \tag{14}$$

When T1 is turned off (Figure 5, $R_{load} = \infty$)

$$V_L = V_G - V_o \tag{15}$$

$$i_C = I_L \tag{16}$$

Using equation 11, equation 13, and the fact that after T1 closes the initial inductor current is $I_o = I_{L,max}$

$$I_L = I_o + \frac{1}{L}\int V_L dt = I_{L,max} + \frac{(V_G - V_o)t}{L} \tag{17}$$

This is a linearly decreasing function as $V_o > V_G$.

If $t_{I=0}$ is the time, after which $I_L$drops to 0,

$$\frac{V_G T_{on}}{L} + \frac{(V_G - V_o)t_{I=0}}{L} = 0 \tag{18}$$

Solving this equation yields:

$$t_{I=0} = \frac{V_G T_{on}}{V_G - V_o} \tag{19}$$

The waveforms of $I_L$and V_L are shown in Figure 7.

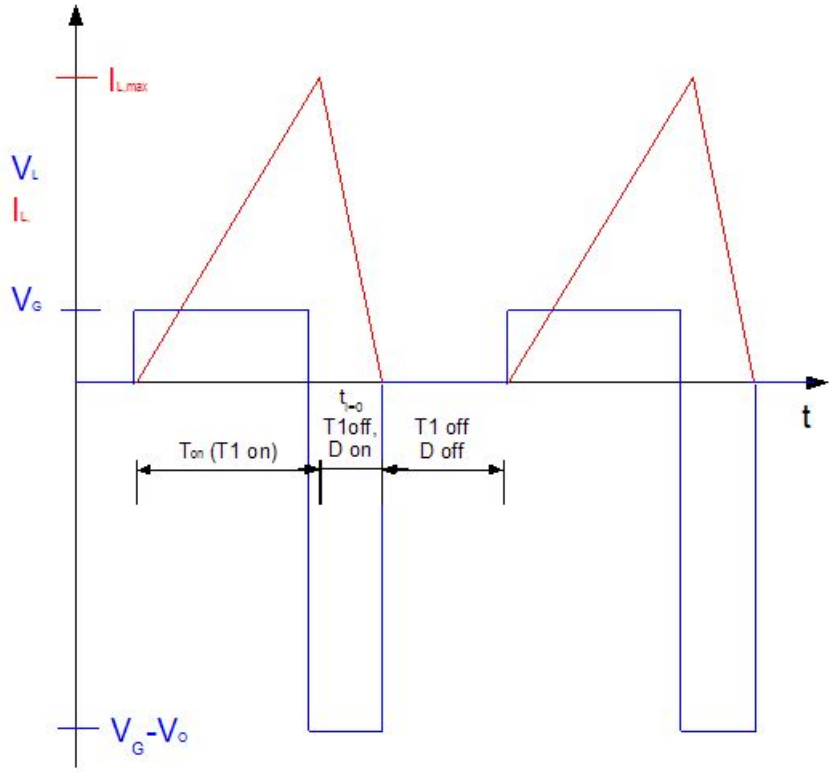

Figure 7: Inductor current and voltage in a boost regulator (no load)

Let's calculate the output voltage of the boost regulator.

According to the differential equation describing the relationship between capacitor current and voltage

$$I_C = C\frac{dV_o}{dt} \tag{20}$$

This means that the capacitor's output voltage rise in each cycle can be expressed as:

$$\triangle V_o = \frac{1}{C}\int_0^{T_s} I_C dt \tag{21}$$

From equation 10 and 16 we know that current only flows in the capacitor while T1 is off:

$$\triangle V_o = \frac{1}{C}\int_0^{t_{I=0}} I_C dt = \frac{1}{C}\int_0^{t_{I=0}} I_L dt = \frac{1}{C}\frac{I_{L,max}t_{I=0}}{2} \tag{22}$$

Substituting equation 13 for $I_{L,max}$and equation 19 for $t_{I=0}$

$$\triangle V_o = \frac{V_G^2 T_{on}^2}{2LC(V_G - V_o)} \tag{23}$$

Let V_{O1} be the output voltage V_o at the beginning of the switching cycle, and V_{O2} after it.

Then

$$\triangle V_o = V_{O2} - V_{O1} = \frac{V_G^2 T_{on}^2}{2LC(V_G - V_{O2})} \tag{24}$$

Solving this equation for V_{O2} yields:

$$V_{O2} = \frac{V_G + V_{O1} + \sqrt{(V_G + V_{O1})^2 - 4(V_{O1}V_G - (\frac{V_G^2 T_{on}^2}{2LC}))}}{2} \tag{25}$$

This equation expresses that the output voltage of a boost regulator with no load rises consistently in each switching cycle from $V_{O1}$to V_{O2}.

Assuming the battery voltage V_G, the duty cycle and the switching frequency (thus T_{on}) are constant during the operation of the boost regulator, then the excess voltage gained in each cycle depends solely from V_{O1}.

It can be shown that the gained excess voltage $\triangle V$ becomes smaller, as the output voltage V_O rises. From equation 23

$$lim_{V_o \to \infty}(\triangle V_o) = lim_{V_o \to \infty}(\frac{V_G^2 T_{on}^2}{2LC(V_G - V_o)}) = 0 \tag{26}$$

The reason for this is that as Vo rises it takes less and less time for the inductor current to drop to 0 ($t_{I=0}$), thus the capacitor will have less and less time to charge.

This can also be shown from equation 19:

$$lim_{V_o \to \infty}(t_{I=0}) = lim_{V_o \to \infty}(\frac{V_G T_{on}}{V_G - V_o}) = 0 \tag{27}$$

The above described behaviour and the resulting equations were also verified by Spice simulations (Figure 8a and 8b).

Now let's consider the behaviour of the stimulator while T2 or T3 is closed, which means that a pulse is currently being delivered.

The boost regulator now 'sees' the skin and tissue resistance as load, and provided the boost converter is stable, the output voltage will move towards its steady state level in discontinuous mode (R_{skin} is too high for the boost regulator to operate in continuous mode). As discussed earlier in this chapter, this steady state output voltage is much smaller, so it is a fair approximation that this process can be described by the exponential discharge of the capacitor through R_{skin} (small ripple approximation can evidently not be used here).

The decline of V_O during the pulse can be estimated by

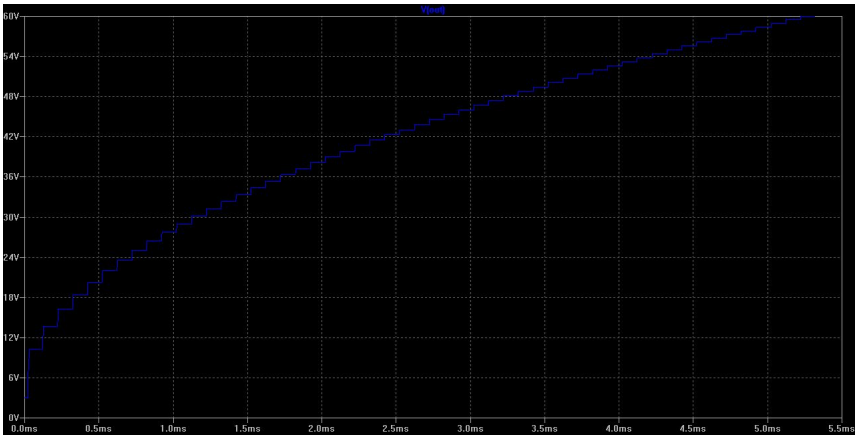

(a) Spice simulation: Boost regulator's capacitor voltage, $V_G = 3V$, L=500 μH, C=0.1 μF, $f_s = 10$ kHz, D=20%. It can be observed that voltage only rises while transistor T1 is off and diode D is on, which results in a step-like waveform

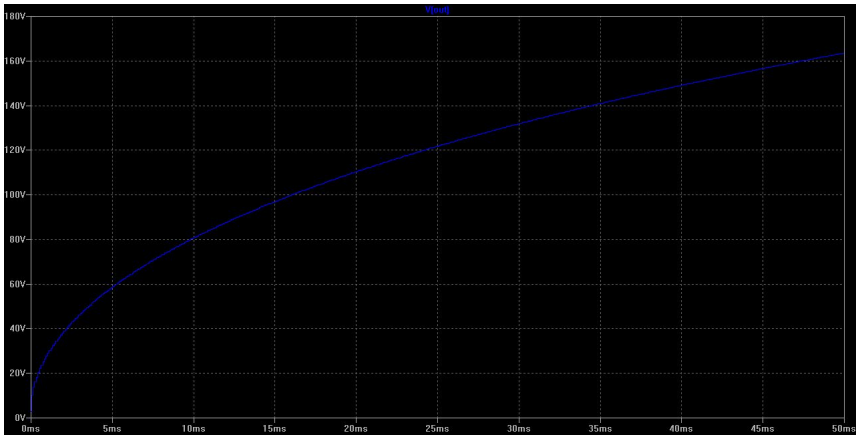

(b) Spice simulation: Boost regulator's capacitor voltage, $V_G = 3V$, L=500 μH, C=0.1 μF, $f_s = 10$ kHz, D=20%. It can be observed that voltage doesn't rise linearly due to the diminishing $t_{I=0}$.

Figure 8: Spice simulations of rising output voltage, if boost converter's load is removed

$$\triangle V_o = -V_{O1} e^{-\frac{T_p}{RC}} \tag{28}$$

Where

T_p is the pulse duration

and U_{O1} is the capacitor's output voltage before the pulse.

The stimulator's output stage in Figure 6 will find its steady state of operation, if the net change in capacitor voltage between pulses is zero (capacitor charge balance [13]), thus the gained voltage between pulses equals the lost voltage during a pulse, expressed in equation 28.

If N switching cycles occur between two stimulation pulses, N can be expresses as

$$N = \frac{T_{pulse} - T_p}{T_s} \tag{29}$$

As a reminder:

T_P is pulse duration,

T_{pulse} is the time interval between two pulses,

T_s is the switching period of the boost converter.

The total inter-pulse voltage gained can be calculated recursively using equation 25:

$$V_{O2} = \frac{V_G + V_{O1} + \sqrt{(V_G + V_{O1})^2 - 4(V_{O1} V_G - (\frac{V_G^2 T_{on}^2}{2LC}))}}{2}$$

$$V_{O3} = \frac{V_G + V_{O2} + \sqrt{(V_G + V_{O2})^2 - 4(V_{O2} V_G - (\frac{V_G^2 T_{on}^2}{2LC}))}}{2}$$

...

$$V_{ON} = \frac{V_G + V_{O(N-1)} + \sqrt{(V_G + V_{O(N-1)})^2 - 4(V_{O(N-1)} V_G - (\frac{V_G^2 T_{on}^2}{2LC}))}}{2}$$

Using equation 28, steady state is achieved if

$$V_{ON} - V_{O1} = V_{ON} e^{\frac{T_p}{RC}}$$

The above described method is an accurate way to determine output voltage of Figure 6 , but it would be very demanding task for a microcontroller. It requires lots of processing power and memory because of the recursive calculations. Therefore, it was not implemented, but it can be used for simulation purposes. Figure 9a shows my Spice simulation, as the circuit in Figure 6 reaches its steady state, and Figure 9b shows the typical waveform of a single pulse in steady state. The decline of the pulse top is an inevitable result of the capacitor's discharge process.

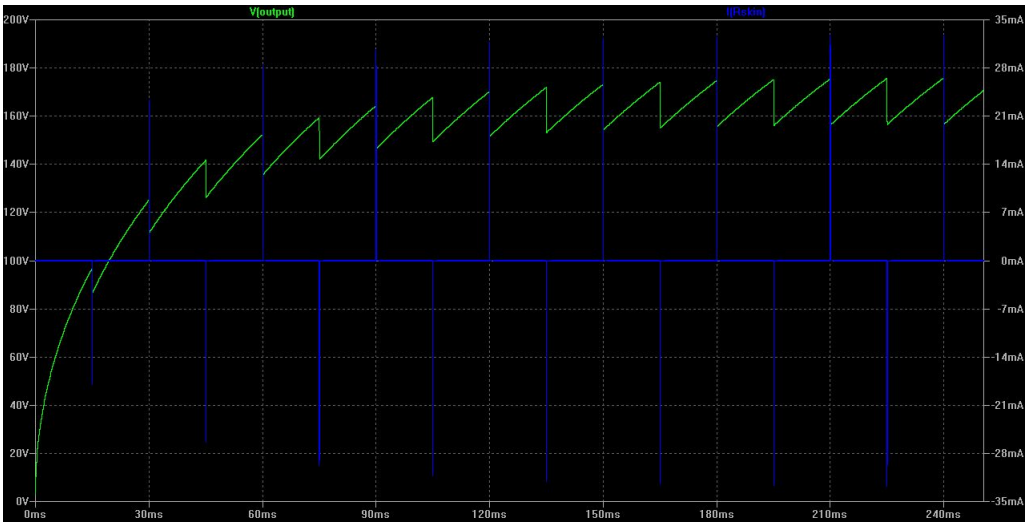

(a) Transient response of output stage, $V_G = 3V$, L=500 μH, C=0.1 μF, R_{skin} = 5kOhm, f_s = 10 kHz, D=20%, $T_p = 50\mu s$, T_s = 15ms, biphasic pulses, Blue - current delivered through patient, Green - output voltage

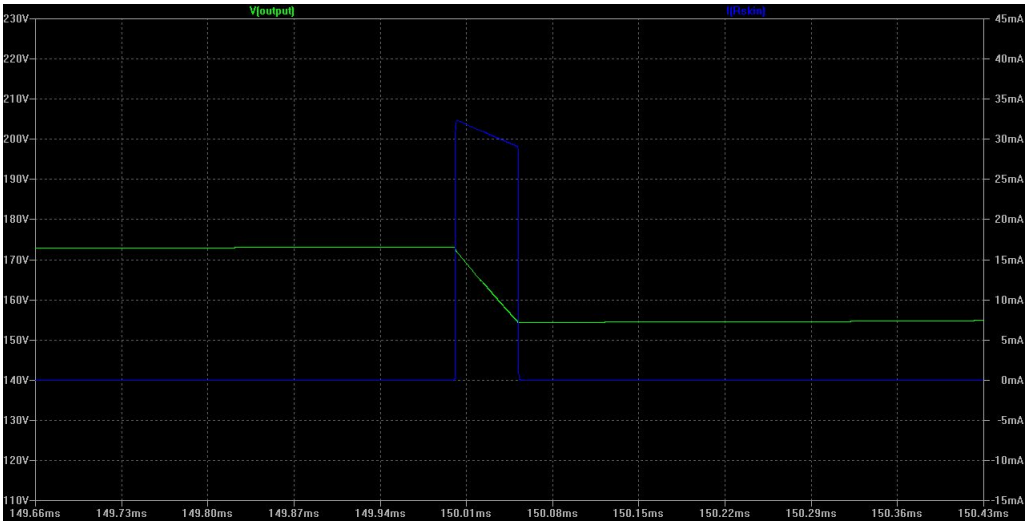

(b) Closeup on a single pulse, $V_G = 3V$, L=500 μH, C=0.1 μF, R_{skin} = 5kOhm, f_s = 10 kHz, D=20%, $T_p = 50\mu s$, T_s = 15 ms. Blue - current delivered through patient, Green - output voltage

Figure 9: Spice simulation of output stage

3.3 Selection of circuit components

The discussion above assumed that all circuit elements are ideal, which is not the case in practice. Keeping the price of the final device down requires some sacrifices when it comes to selecting the right parts. The following discussion examines what key component characteristics needed extra attention during this design step [13].

- Switching frequency

High switching frequencies must be generally avoided, as switching losses drastically reduce the efficiency of the power conversion. On the other hand increased switching frequencies also enable the converter to reach higher output voltages with lower duty cycles, reducing the maximal current flowing in the inductors. The time to reach steady state operation also becomes faster. Empirically 5.7 kHz was found to be optimal.

- Transistor

In a regular boost converter operating in continuous mode usually a MOSFET is suggested as it has superior switching times compared to bipolar junction transistors (BJT). In that case, increasing the switching frequency can reduce the voltage ripple even with smaller inductors and capacitors. For the stimulator output stage these issues were less relevant, therefore a BJT was used, which exhibits lower forward voltage drop and higher breakdown voltage at lower price. This stimulator's output voltage was designed not to exceed 300 V and the transistor's breakdown voltage was chosen accordingly.

- Inductor

It is crucial for the inductor to have a higher peak current rating than $i_{L,max}$, which can be calculated from equation 13. With improper design the inductor might overheat or saturate, if duty cycles are pushed too high. Lower inductances cause output voltage to rise more rapidly (see equation 25), because they also increase the total transferred charge in each cycle, and thus also $i_{L,max}$. For my design L=2.2mH was chosen with a peak current rating of 0.25 A. The series resistance of the inductor also introduces losses, although these are only dominant at high duty cycles. Therefore, in this design series resistance of the inductor is not a crucial point to consider.

- Diode

For high switching frequencies the rectifier's reverse recovery time must be small, as exhibited by Schottky diodes and Fast recovery rectifiers. Forward voltage drop must also be kept low in order to achieve high efficiency power conversion. Attention must be paid, that the reverse breakdown voltage is higher than the maximum output voltage, and $i_{L,max}$ (which is also the maximal diode current) doesn't exceed the peak current rating.

- Capacitor

Lower capacitances cause output voltage to rise steeper (see equation 25), but they also cause a more rapid decline of pulse tops. Apart from this, high equivalent series resistance introduces losses and thus reduces efficiency. Lastly, the maximum voltage rating must be higher than 300 V (or the appropriate maximal output voltage).

The selected components can be found in the Appendix under the section Bill of materials.

3.4 Current consumption

The current consumption of the stimulator in Figure 6 can be determined by calculating the average inductor current in one switching cycle.

$$< I >=< I_L >= \frac{1}{T_s} \int_0^{T_s} I_L dt \tag{30}$$

Using Figure 7 we can calculate the area of the triangles instead of integration:

$$< I_L >= \frac{1}{2T_s}(I_{L,max} T_{on} + I_{L,max} t_{I=0}) \tag{31}$$

With equation 13 to determine $I_{L,max}$ and equation 19 to determine $t_{I=0}$

$$< I_L >= \frac{1}{2T_s} \frac{V_G T_{on}}{L}(T_{on} + t_{I=0}) = \frac{1}{2T_s} \frac{V_G T_{on}}{L}(T_{on} + \frac{V_G T_{on}}{V_G - V_o}) \tag{32}$$

Because V_o changes in each cycle the current consumption of the circuit will change as well (see Figure 9a). It will peak before the pulse is delivered, and the lowest amount of current will be required when the circuit is switched on.

3.5 Closed loop control

As mentioned at the end of chapter 3.2, no simple explicit equation was found for the output voltage of the stimulator device. Even if this wouldn't be an issue, the skin and tissue resistance of the patient under therapy varies in broad range. For these reasons, the presented device would not yet be capable to deliver current pulses with given amplitudes.

As a solution, closed loop control (Figure 10) will be introduced to regulate the output voltage of the boost converter.

Current through the skin will be measured across a resistor and fed back to the analog-digital converter (ADC) of the microcontroller (MCU). The MCU will calculate the error signal, apply the controller transfer function and generate a PWM signal to drive the switching transistor of the boost regulator (as it was discussed in section 3.2, the output voltage increases as the duty cycle of the PWM is increased). Since current will only flow through the resistor during pulses, the sampling and updating of the PWM can only take place at the rate

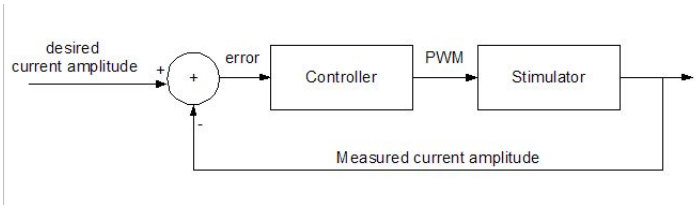

Figure 10: Block diagram explaining the closed loop control of the boost converter

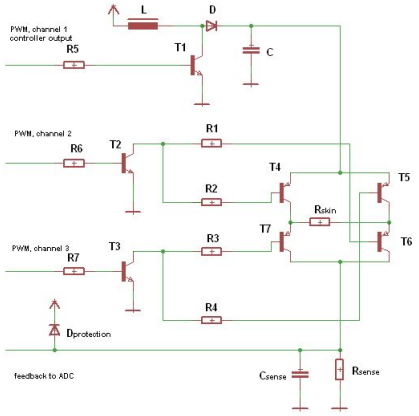

Figure 11: The complete output stage of the stimulator

of the pulse repetition frequency, f_{pulse}. This is not an issue, the time constant of the controlled system is relatively high, it might take several pulses until steady state is reached (Figure 9a).

The final schematic of the stimulator's output stage can be seen in Figure 11.

As current pulses flow through R_{sense} to ground, a proportional voltage will appear on the input of the ADC. C_{sense} damps the rising overshoot from U_{sense} (the feedback for the ADC) and $D_{protection}$ protects the microcontroller from high voltage spikes. Sampling will take place in the middle of the pulse from the average of the exponentially declining pulse top. This approach can drive close to ideal amount of charge through the tissue.

The upper level of ADC conversion (full scale) is 2.5 V, and the maximal current amplitude is 125 mA, therefore$R_{sense} = 20$ Ohm was chosen.

The controller will be a digital integral controller. Its software implementation will be explained in section 5.1.

4 Wireless communication

One of the most distinctive features of the surface stimulator in this project was that it must be controlled over a wireless communication channel from a PC. There were several ICs as candidates for this task, but finally Chipcon AS's (subsidiary of Texas Instruments) CC1000 transceiver chip was selected.

4.1 CC1000

The following discussion will describe the relevant features of the chosen wireless transceiver based on [21], [22], and [25]. The layout of the wireless chip and its external components was made based on [23] (it can be found in the Appendix).

The CC1000 features extremely low power consumption compared to its alternatives due to Chipcons's 350 nm CMOS SmartRF® technology. Combined with the ultra low power MSP430 microcontroller (to be discussed later) it can provide extended battery lifetime which was crucial in my application. Furthermore, contrary to TI's newest sub 1 GHz CC1101 chip, the CC1000 is available in a 28 pin Thin-Shrink Small Outline Package (TSSOP) which can be soldered manually.

The CC1000 can transmit data in the ultra high frequency (UHF) radio band from 300 MHz to 1 GHz. In Europe the 433 MHz and the 868 MHz ISM (Industrial, Scientific and Medical) bands are available for customer specific radio transmission without a licence[14], from which the 433 MHz band was selected, as it allows extended working range and reduced power consumption (see Table 2). Its drawback is the longer antenna required for the perfectly matched condition, but with the adjusted output power of P=0 dBm, sub-optimal design should also comply with the specified working range (the whole system should be kept in a room). If extended reach will be needed one can easily increase the output power to 10 dBm, but only at the cost of increased consumed power. Nevertheless this rise shouldn't be significant, as I put overwhelming effort in tailoring a current consumption profile which keeps the IC in power down mode during most of its operation time.

	433 MHz	866 MHz
Receive mode	7.4 mA	9.6 mA
Power down mode	200 nA	
Transmit mode / P=-20 dBm	5.3 mA	8.6 mA
Transmit mode / P=-5 dBm	8.9 mA	13.8 mA
Transmit mode / P=0 dBm	10.4 mA	16.5 mA
Transmit mode / P=5 dBm	14.8 mA	25.4 mA
Transmit mode / P=10 dBm	26.7 mA	N/A

Table 2: Typical current consumption of the CC1000 [21]

The CC1000 uses frequency shift keying (FSK) to modulate the incoming

digital datastream into radio waves.

FSK systems vary the frequency of the carrier wave to represent binary ones and zeroes:

$$s_m(t) = Acos(2\pi t(f_c \pm f_D)) \tag{33}$$

Where
$s_m(t)$is the modulated signal
A is the amplitude of the modulated signal
$f_c$is the carrier wave frequency and
$f_D$is the frequency deviation

One of the unpleasant property of the FSK modulation is that the modulated signals' theoretical bandwidth is infinitely wide, which means that it cannot be transmitted in a bandlimited channel. Fortunately however most of the spectral components are found in a band near the carrier frequency, as can be seen from Figure 13[21]. The practical bandwidth of the power spectrum was estimated using Carson's rule[15]:

$$B = 2(f_D + F_m) \tag{34}$$

Where
$f_D$is the frequency deviation
$F_m$is the modulation frequency.

The parameters of the system are stored in a control register block, which can be read and modified by a 3-wire serial interface, comprising of PDATA, PCLK, and PALE. I used TI's SmartRF Studio software to calculate the contents of the configuration registers for my specified transmission band.

The operation of the CC1000 can be understood from its block diagram in Figure 12:

According to their function we can distinguish three parts of the system[21]:

- The frequency synthetiser and FSK modulator
- The receiver
- and the transmitter

The frequency synthetiser consists of a voltage controlled oscillator (VCO) and a phase locked loop (PLL) circuit which receives its reference signal from a stable external crystal oscillator running at 14.7456 MHz. Apart from that, all blocks of the PLL and VCO, including the phase detector, the charge pump, and the frequency dividers (/N, /R) are integrated on the chip, with the only notable exception of the external inductor of the VCO. This component was found very crucial to be precisely tuned to the center frequency, otherwise the PLL would not be able to lock. This is only achievable with an inductor with L=33 nH, featuring high Q factor and low tolerance. It must also be noted that the PLL is very sensitive to temperature and supply voltage variations,

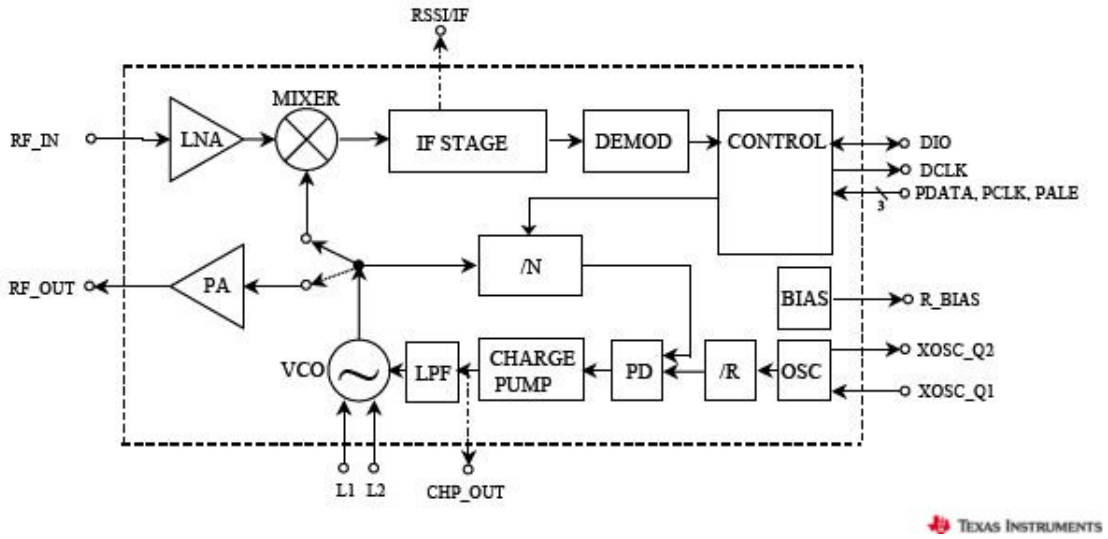

Figure 12: Block diagram of the CC1000 [21], with permission of TI

for which it must be calibrated at startup. This can be done automatically by issuing the appropriate command to the control registers.

In transmit mode the PLL multiplies the crystal oscillator's low frequency to generate the modulated radio signal by setting the frequency dividers of the PLL. The configuration registers have to be previously programmed to contain the parameters of the FSK modulation, such as $f_c = 434.092$ MHz center frequency and $f_D = 32$ kHz frequency deviation, which is the maximum adjustable value. Keeping the frequency separation high increases the sensitivity of the receiver, but also broadens the bandwidth. With a bitrate of 9.6 kbit/s we can use Formula 34 to calculate the practical bandwidth of the system, which is 83.2 kHz. The resulting transmitted power spectrum can be seen in Figure 13. We can see that the whole occupied frequency region is within the ISM band.

The modulated signal is fed to the power amplifier of the transmitter whose amplification was set to 0 dBm by software.

As receiver the CC1000 follows the superheterodyn principle, thus after a low noise amplifier the modulated radio signal is converted down to an intermediate frequency (IF) of 150 kHz. The local oscillator signal of the mixer is generated by the frequency synthetiser. The IF signal is then amplified and the unwanted frequency components are removed by an internal IF filter after which the demodulator recovers the digital data stream on the DIO line. Data decision and synchronisation are also provided on chip, the falling edge clock signal on DCLK will indicate valid data on DIO. This can ease the workload of the microcontroller considerably since it can trigger external interrupts on signal transitions of DCLK.

In order to synchronise data precisely the CC1000 encodes the incoming Non-

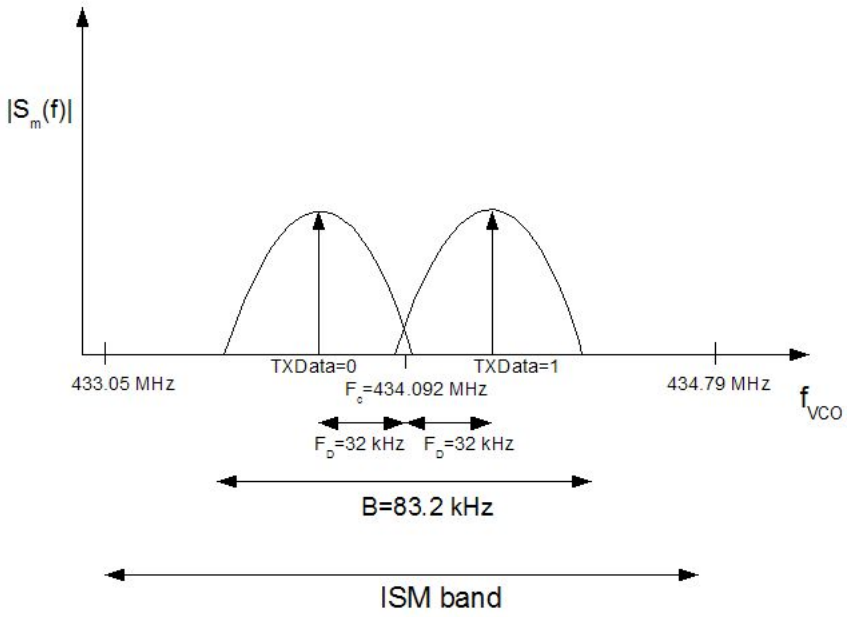

Figure 13: Transmitted power spectrum of the FSK modulated system, rough estimation

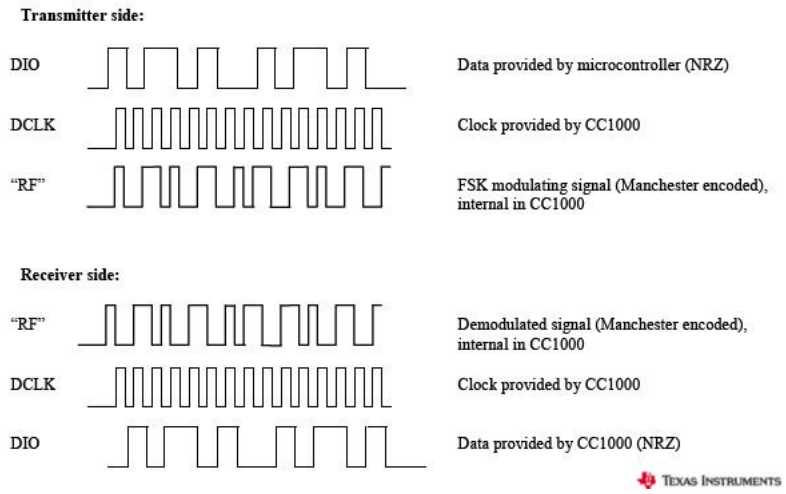

Figure 14: Synchronous Manchester encoding [21], with permission of TI

Return-To-Zero (NRZ) datastream into Manchester code before modulation, which ensures that there will be at least one signal transition during each bit period and keeps the datastream DC balanced[21].

Keeping the signal DC balanced helps to find the correct threshold value for the data slicer in the demodulator. This threshold value is presented by an averaging filter which was set to be free running in the properly DC balanced Manchester encoded datastream. Nevertheless every data packet should start with at least four bytes of alternating 1s and 0s, otherwise the sensitivity for a given bit error rate (BER) would be greatly reduced. The application's data rate, center frequency, frequency separation and preamble length together predict the sensitivity of the receiver, which is -104.7 dBm for BER=10^{-3}.

The CC1000 has half duplex communication capability, but in this project only simplex communication was required by the unidirectional data flow from the PC to the stimulator. This could keep the embedded software simpler, and it allowed for a more efficient power management (see section 5.1.2). The data rate was set to be 9600 bit/s, but it could be amended to 38.4 kbit/s or even 76.8 kbit/s if we turned off Manchester encoding (which uses twice as much bandwidth as NRZ). In this application this was also unnecessary as very small amount of data is to be transmitted, but both of these features might be useful if data acquisition functionality was to be added in the future (see section 8).

4.2 Antenna design

The employed antenna is a meandering monopole radiator integrated onto the PCB, similarly to a transversal helix antenna. [16] suggests that such design should go as long as possible perpendicular to the ground plane, otherwise parasitic capacitance to ground and inductance due to bends will be introduced,

which reduce the efficiency. Unfortunately considering this guideline would have meant an intolerable increase in circuit board area, thus, again the optimum working range was to be traded for reduced size.

The ideal length of a monopole antenna in free space must be one quarter of the electrical wavelength, which is

$$L \approx \frac{\lambda}{4} = \frac{c_0}{4 * f} = \frac{3 * 10^8}{4 * 434 * 10^6} \approx 17.3cm \tag{35}$$

Where
L is the length of the antenna
λ is the electrical length
c_0 is the speed of light in free space
and f is the frequency of the signal

The actual length of the antenna on the design was shorter (approximately 13 cm), which can be justified by the fact that PCB has a dielectric constant $\varepsilon_r > 1$, subsequently light propagates slower which results in a shorter ideal antenna length (see equation 35). Nevertheless the optimal length could only be determined by measuring the antenna impedance with a vector network analyser, and fine tuning the radiator length, the matching inductor and matching capacitor values until efficiency is maximalised[16].

5 Overall system description

The complete wireless stimulation system consists of the following blocks:

- Personal Computer / Laptop

The therapist can remotely configure the stimulator from a PC equipped with an RS232 serial port, which issues the desired commands through the serial cable to the RS232/wireless interface board.

- RS232/Wireless Interface board

It receives the commands from the PC through its serial interface, organizes the incoming bytes into packets and transmits them to the stimulator wirelessly.

- Wireless stimulator

It performs neuromuscular stimulation and receives the stimulation parameters over a radio frequency link from the RS232/Wireless Interface board.

Figure 15: The wireless stimulation system

Two circuit boards needed to be designed for this project, that of the wireless stimulator and that of the RS232/wireless interface. In the following sections, they will be discussed independently.

5.1 Wireless stimulator

5.1.1 Hardware description

The block diagram of the wireless stimulator is shown in Figure 16. The microcontroller handles configuration and data exchange with the CC1000 chip over a serial interface. It controls the stimulator output stage with its PWM channels and processes the feedback. It alerts the user with an LED, if stimulation is in progress.

Microcontroller selection

The MSP430F2122 is a relatively cheap, yet powerful mixed signal microcontroller (MCU) from Texas Instruments with extremely low power consumption, which makes it suitable in portable, battery powered applications[18, 17, 19]. It features a 16 bit RISC architecture, which together with its adjustable, maximum 16 MHz internal crystal oscillator facilitates fast instruction execution

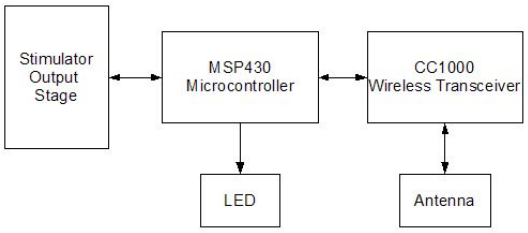

Figure 16: Block diagram of wireless stimulator

times. Several peripherals are integrated on chip (Figure 17), including two 16 bit Timers, suitable for generating two independent PWM channels for the stimulator's output stage, an Universal Serial Communication Interface (USCI) which can be configured to receive serial data in UART format from the RS232 port of the PC, and a fast 10 bit successive approximation analog-to-digital converter (ADC), which can directly digitalise the feedback of the digital controller.

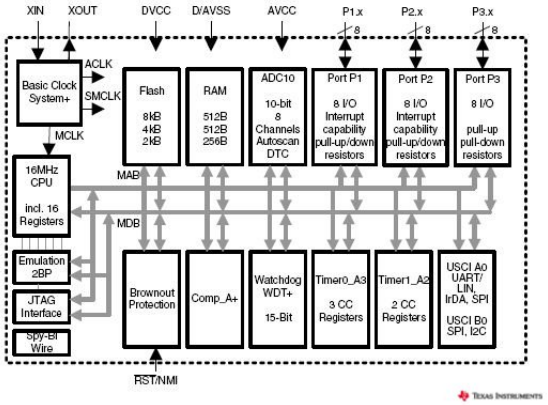

Figure 17: Functional block diagram of the MSP430F2122 microcontroller[17], with permission of TI

The IC's power consumption is2.4 mA at 8 MHz, but it can be reduced to 560 μA by turning the MCU to low power mode LPM0. Thanks to a versatile clock system waking up from low power mode to active mode is extremely fast and easy compared to other microcontroller families[19].

This MCU has up to 24 GPIO pins of which only six are needed, five for interfacing with the CC1000 chip and one for the LED. Some other pins were assigned to active peripherals, such as the Timer, and the ADC.

The MSP430F2122 has 512 Bytes of integrated SRAM and 4 kB of Flash memory. The latter can be upgraded to 8 kB by replacing the chip to the MSP430F2132 variant, whose internal features match the MSP430F2122 except

for the extended Flash.

The MCU is available in a small, 28 pin Thin-Shrink Small Outline Package (TSSOP), which could be soldered manually at the university.

Development tool

The MSP430F2122 was programmed and debugged with the MSPFET430UIF Flash Emulation Tool (FET) via 2-wire JTAG (Spy-Bi-Wire) communication. I built a programming interface board (its schematic can be found in the Appendix) which included a standard 14 pin JTAG connector and all external components and signal connections which are only necessary for successful programming, but not for the correct operation of the device, after the programmer was detached. The stimulator and the RS232/Wireless interfacing board can be programmed after the MSPFET430UIF pod is connected to the JTAG connector andthe necessary connections are made with the programmed board. The target board's power is supplied from the pod, therefore any on-board battery must be deactivated.

Wireless communication

The CC1000 wireless transceiver chip has a 3-wire serial configuration interface and a 2-wire serial data interface. Five GPIO pins of the microcontroller are dedicated for handling communication with these interfaces using a technique called 'bit banging'. At the data rate of 9.6 kbit/s the extra workload is negligible for a powerful microcontroller, like the MSP430[22]. A more detailed discussion about the CC1000 chip can be found in Section 4.1.

Power supply

The MSP430F2122 MCU's supply voltage spans from 1.8V-3.6V, while that of the CC1000 wireless transceiver ranges from 2.1-3.6V. With this in mind, a 3V 2032 Lithium Battery was chosen as power supply, which is situated on the back side of the PCB. From such a battery the MCU can only run reliably with CPU frequencies at 8 MHz. (It must be mentioned, that there is no voltage regulator on the design, which means that the supply voltage will decline with the aging of the battery. According to [17] both the MCU at 8 MHz and the CC1000 chip can work reliably with supply voltages over 2.2 V, which was considered a fair safety margin.) With the MSP430F2122's powerful RISC architecture I found 8 MHz of master clock frequency acceptable for this application, and the reduction of processing speed also reduced the current consumption of the IC.

5.1.2 Software description

One of the highlights of the MSP430 microcontroller is the ease, by which it can switch between active mode and low power mode[19]. In order to utilise this feature I assigned most of the tasks to peripherals, which trigger interrupts to

wake up the microcontroller from low power standby mode if needed. The main tasks that had to be handled by software were the following:

- The PWM channels of the stimulator output stage could be generated entirely by the two Timers, the CPU only has to intervene if the stimulation parameters need to be updated. The digital controller's algorithm could be also triggered by one of these Timers.
- The communication with the CC1000 chip could be triggered by the external interrupts of the wireless transceiver benefitting from the data synchronisation mechanism it employs. In order to reduce the power consumption of the CC1000 chip it is kept in power down mode most of the time, and it is woken up regularly to check for valid traffic. This technique is called polling[22]. As all regular timers were busy generating PWM for the output stage, I had to reconfigure the Watchdog Timer (WDT) to schedule the polling. The WDT was also used for timing the blinking of the LED after system startup.

As we can see, after the system initialisation the code architecture is completely interrupt driven according to the recommendation of TI [24]. However, the interrupt service routines (ISR), especially that of the CC1000 communication handling are fairly long, and no interrupt nesting is supported. As a result, some interrupts may never be served. TI recommends to handle all interrupts in the main loop, the ISR should set a flag according to what action needs to be taken and only execute code which is urgent[24].

The flowchart of the main() function in Figure 18 demonstrates this concept.

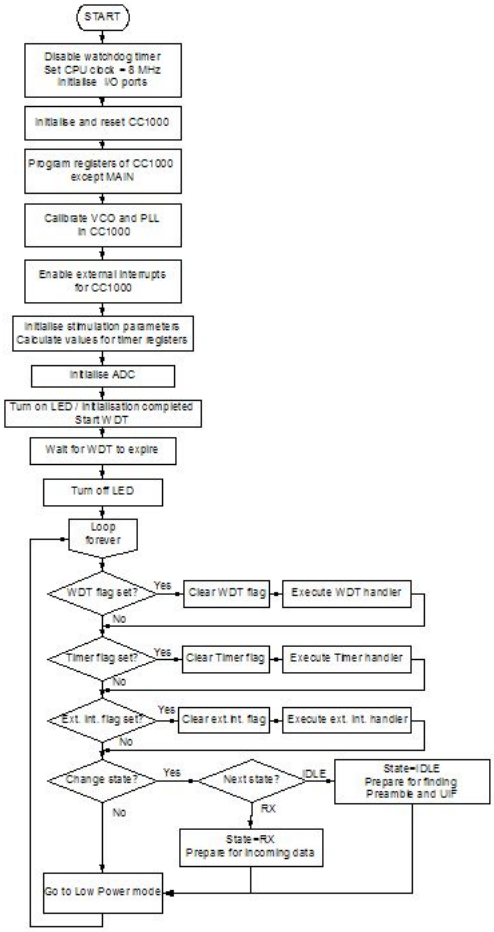

Figure 18: Main() function of wireless stimulation software

The boost converter and Timer_A1

The PWM for the switching transistor of the boost converter was generated with one of the MSP430 microcontroller's general purpose 16 bit timers, Timer_A1.

It's Timer/Counter register (TAR) was configured to increment from 0 up to the value in the first channel of capture/compare registers (TACCR0), then jump back to zero (see Figure 19a.). The counting was triggered by the rising edge of the 8 MHz digitally controllable oscillator (DCO). If the content of TAR equals TACCR1 (the second channel of capture/compare registers), a compare event occurs, which updates the PWM output without the need for software intervention. This provides very precise timing.

As it can be seen in Figure 19a, the frequency of the output signal is determined by TACCR0, and the duty cycle by TACCR1.

It was already mentioned, that the boost converter's optimal switching fre-

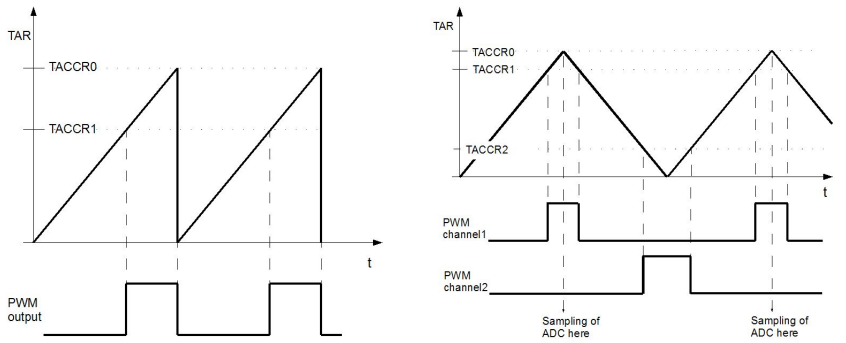

(a) The output of Timer_A1 in Up mode (b) The outputs of Timer_A0 in Up/Down mode

Figure 19: PWM generation of Timer_A1 and Timer_A2

quency (f_{SW}) was found to be 5,7 kHz. This is a relatively low value in order to reduce switching losses and increase the resolution of the duty cycle that can be set.

The contents of TACCRx can be calculated as follows:

$$TACCR0 = \frac{f_{SMCLK}}{f_{sw}} - 1 = \frac{8MHz}{5{,}7kHz} - 1 \approx 1400$$

and the duty cycle can be calculated as:

$$D = \frac{TACCR1+1}{TACCR0+1}$$

Pulse width of stimulation current and Timer_A0

Timer_A0 provides the timing of the negative and positive stimulation pulses. It has three Capture compare registers, but channel 0 (TACCR0) is lost for setting the upper limit for counting, which determines the frequency. The two remaining channels can set the duty cycle for each PWM output. Like Timer_A1, Timer_A0 is clocked from the internal 8 MHz DCO, but this time the master clock is divided by 8 (f_{SMCLK}), since the frequency of stimulation pulses is lower that the frequency of switching in the boost regulator.

The timer is operated in Up/Down mode, where the counter counts from 0 up to TACCR0 (capture/compare register for channel 0), then back to zero. Centered pulse width modulation (Figure 19b) allows the ADC to sample at the center of the pulse, from the mean of the decaying pulse top, avoiding transients. Another advantage of the Up/Down mode is that as long as TACCR1>TACCR2, both outputs cannot switch on at the same time, which protects the stimulator in Figure 11 from a short circuit caused by opening T4, T5, T6 and T7 at once.

The duty cycle can be calculated as

$$D1 = \frac{2TACCR0}{2TACCR1}, \text{ and } D2 = \frac{2TACCR0}{2TACCR12},$$

and the frequency of pulse repetition is

$$F_p = \frac{f_{SMCLK}}{2TACCR0}.$$

The frequency of the sub-master clock is 1 MHz, and TACCR0 is a 16 bit register, which limits the lowest achievable pulse repetition frequency to 8 Hz. This sets no major limitation to the device, because functional electrical stimulation is rarely performed at frequencies below 12 Hz[5]. It is possible to decrease this limit by sourcing the timer from the very low frequency oscillator (VLO), but it is not recommended because measurements suggested that the stimulator output stage behaves unreliably below the frequency of 25 Hz (see Section 6).

Again, the output of the PWM is directly connected to the Timer for precise timing, which produces the periodic output without software intervention as soon as a compare event happens (TAR=TACCR1 or TAR=TACCR2) .

Closed loop control and the Analog-Digital Converter

I implemented a digital Integral controller to regulate the stimulation current. The feedback (Figure 10 and 11) is sampled in the interrupt service routine of Timer_A0, which is called on the compare event TAR=TACCR0 (see Figure 19b). The rest of the routine is executed in the main loop.

The current is measured across a 20 Ohm resistor. The feedback voltage can be calculated by

$$V_{in} = 20I_{stim} \tag{36}$$

The analog-digital converter (ADC) is a 10 bit analog successive approximation ADC.

It has the transfer function

$$N = 2^{10}\frac{V_{in} - V_{R-}}{V_{R+} - V_{R-}} \tag{37}$$

where V_{R+} is the upper(2.5V) and V_{R-} is the lower limit (Vss) for conversion[18].

Substituting Equation 36 into Equation 37 yields:

$$N = 2^{10}\frac{20I_{stim} - 0}{(2.5 - 0)} = \frac{1024 * 20}{2.5}I_{stim} = 8192I_{stim} \tag{38}$$

Using this Formula a desired current amplitude can be translated to a desired ADC result (the unit of I_{stim}must be Amps).

Besides the digital controller implementation for constant current stimulation, current measurement also helps eliminating important safety hazards. It can spot a short or open circuit between the electrodes, by comparing N with threshold values (too low or too high current). In either case it immediately stops the stimulation.

The flowchart of the algorithm can be seen in Figure 20.

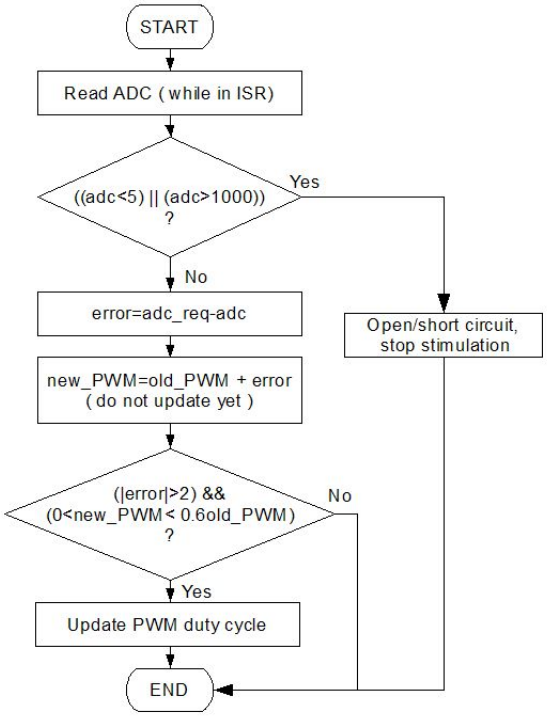

Figure 20: Algorithm for implementing the digital controller

Field	Length in bits	Usage
Preamble	800	Alternating 0s and 1s
Start of Frame Identifier	8	synchronisation word, it must be 0x33
Packet type	8	'S' for Start, 'E' for Stop, 'U' for Update packets
Data	48	Only implemented for 'Update' packets

Table 3: Packet format

Byte Index	
1.	current amplitude
2	MSB of pulse width (positive pulse)
3	LSB of pulse width (positive pulse)
4	MSB of pulse width (negative pulse)
5	LSB of pulse width (negative pulse)
6	pulse frequency

Table 4: Data Field of 'Update' packets

Wireless communication

In order to reduce power consumption, the CC1000 chip is kept in power down mode, and awakened at regular intervals looking for data. The Watchdog Timer (WDT) measures the time until the CC1000 has to be woken up. The polling period was set to 50 ms. Such time intervals are too low for the 8 MHz DCO, so the internal 12 kHz 'Very low power, low frequency oscillator' (VLO) had to be used as clock source instead.

This algorithm requires a supporting communication protocol [25], which is given in Table 3.

Each packet must start with a 100 bytes long preamble containing alternating ones and zeros. When used with Manchester encoding (see section 4.1), Chipcon recommends a minimal preamble length of 98 bits (for best sensitivity) [21]. In order to comply with this, it must be ensured that at least 98 preamble bits are received after the CC1000 chip wakes up, subsequently the length of the preamble (in time) has to be 98 bits longer than the polling period (50 ms). At the data rate of 9600 bit /s, this means the preamble must contain at least 578 bits. The large safety margin was left due to the inaccuracy and thermal instability of the VCO (its actual frequency may vary between 4 and 20 kHz)[19]. The end of the preamble is indicated by the Start of Frame identifier.

All data packets contain a command which depends from the 'Packet type' Field - the 'Start' message initiates neuromuscular stimulation for the patient, the 'Stop' packet turns it off and the 'Update' message updates all stimulation parameters with the contents of the Data field (Table 4).

The software responsible for handling communication with the CC1000 was written as a state machine with two possible states. In IDLE state it monitors the incoming datastream looking for valid data packets (Preamble followed by

start of Frame identifier). If a valid packet header is detected, the program enters RX state, otherwise after a couple of failed attempts the CC1000 is put to standby mode. In RX state the microcontroller extracts data from the packets, analyses them and acts accordingly (turn on/off stimulation, or updates parameters).

The CC1000 chip provides data synchronisation. An external interrupt can trigger on the rising edge of DCLK, and apart from reading the valid data from the DIO line all further handling is done in the main loop (see the whole algorithm in Figure 21).

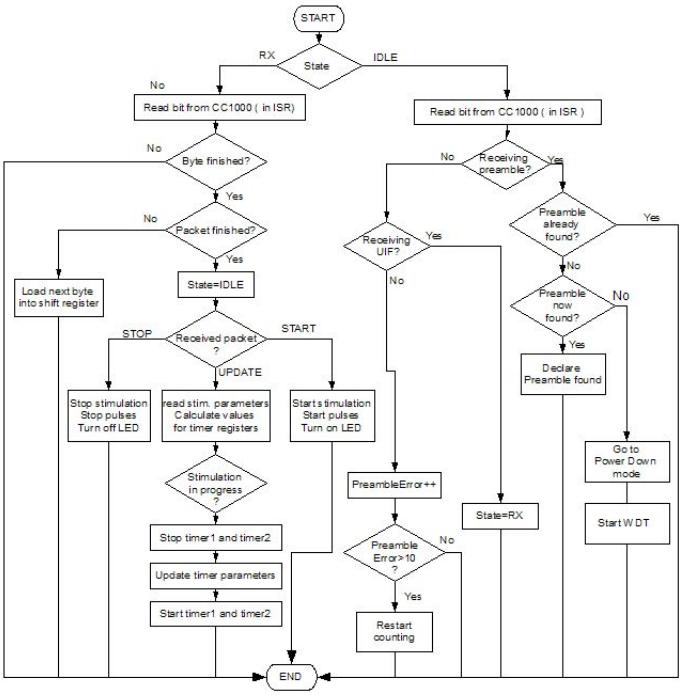

Figure 21: Flowchart of the wireless communication handling

Development environment

The code for the microcontroller was written in C programming language, and the development environment was the MSPGCC Toolchain, an open source project to port the GCC (GNU Compiler Collection) toolchain for the MSP430 family. It includes the GNU C compiler and its libraries, the assembler, the linker (binutils), and the debugger (GDB)[20].

Source files

Table 5 lists and describes the source code files of the software

File name	Description
main_rx.c	Contains the main program
cc1000msp.c	Function library for the CC1000 based on [22]
cc1000.h	Header file for cc1000msp.c
delay.c	Contains functions to delay program execution
delay.h	Header file for delay.c

Table 5: Source files of the software

5.2 RS232/Wireless interface

5.2.1 Hardware description

Figure 22 shows the block diagram of the RS232/Wireless interface board. The MSP430 microcontroller (described in Section 5.1.1) communicates with the RS232 port of the PC. It creates packets from the incoming data and transmits them to the stimulator board over the wireless link. Due to incompatibility of the voltage representation of logical values between the RS232 standard and the MSP430, a MAX3232 chip had to convert the incoming signal to the 3 V standard CMOS voltage level. The incoming serial data is handled by the Universal Serial Communication Interface (USCI) of the MSP430 in UART mode. The microcontroller must also monitor the state of the button and, in case it was pressed, act accordingly (send commands to the stimulator, operate LED).

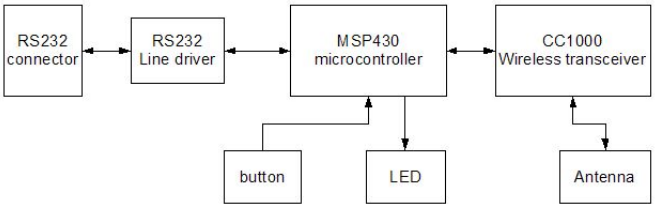

Figure 22: Block diagram of RS232/Wireless interfacing board

About the microcontroller, the wireless transceiver and the development tool please refer to Section 5.1.1.

Power supply and current consumption

The size of the interface board was not a critical factor. This allowed me to use two bulky AA batteries, which are situated on the back side of the PCB. The limitations on CPU frequencies still apply (see Section 5.1.1), the master clock is sourced from the 8 MHz DCO.

5.2.2 Software description

About the development tool and source files please refer to Section 5.1.2. The main program is now called main_tx.c

Main() function

The program flow of the main() function can be seen in Figure 23. I applied the very same software coding principles, which were emphasized in section 5.1.2. The MSP430 initialises the clock, the I/O ports, the peripherals (Timer_A0 for polling the button and the Universal Serial Communication Interface for receiving incoming serial data), and the CC1000 wireless transceiver, which is immediately set to power down mode. The endless loop keeps the microcontroller in low power mode, until an interrupt wakes it up. Again, the interrupt service routines use flags to communicate with the main loop, where most interrupt handling takes place.

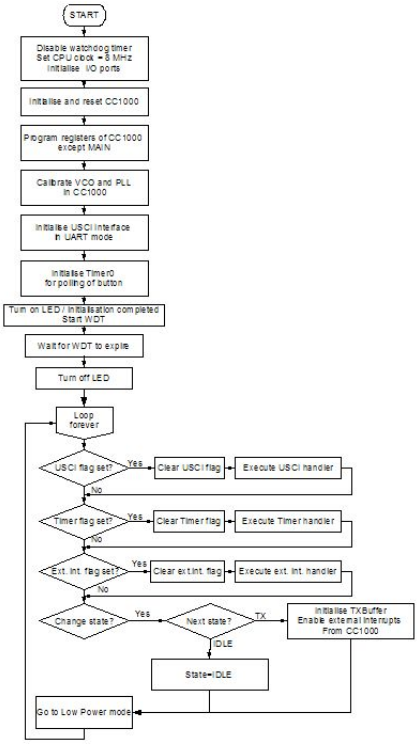

Figure 23: Flowchart for Main() function of Interfacing board

Wireless communication

The program has two states: in IDLE state there is no data to transmit, the microcontroller waits in low power mode, until a packet arrives from the PC or the button is pressed. If either of these events occur, the program enters TX state, wakes up the CC1000 and starts sending the individual bits (see algorithm in Figure 24) on the external interrupts triggered by the falling edge of DCLK.

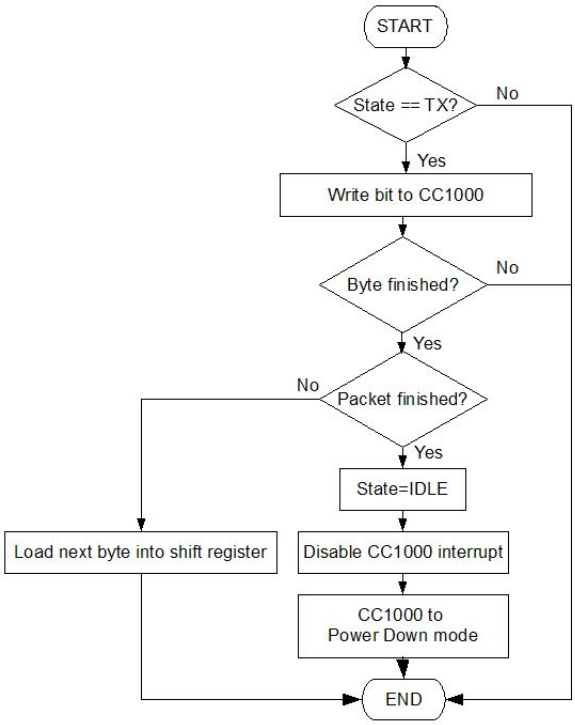

Figure 24: Flowchart of external interrupt handling in the main loop

Polling of Button and TIMER_A0

Timer_A0 polls the button regularly in every 40 ms. This is a suitable interval for debouncing, and it also allows the microcontroller to stay in standby mode. If the button is pressed, the program creates and sends a 'Start' packet. As soon as the button is released, a 'Stop' packet is transmitted to the stimulator module. The MCU keeps the LED on while the button is pressed, indicating that button triggered stimulation is in progress. This feature enables the RS232/wireless interface board to be used as remote controller for stimulation. Figure 25 shows the flowchart of the described algorithm.

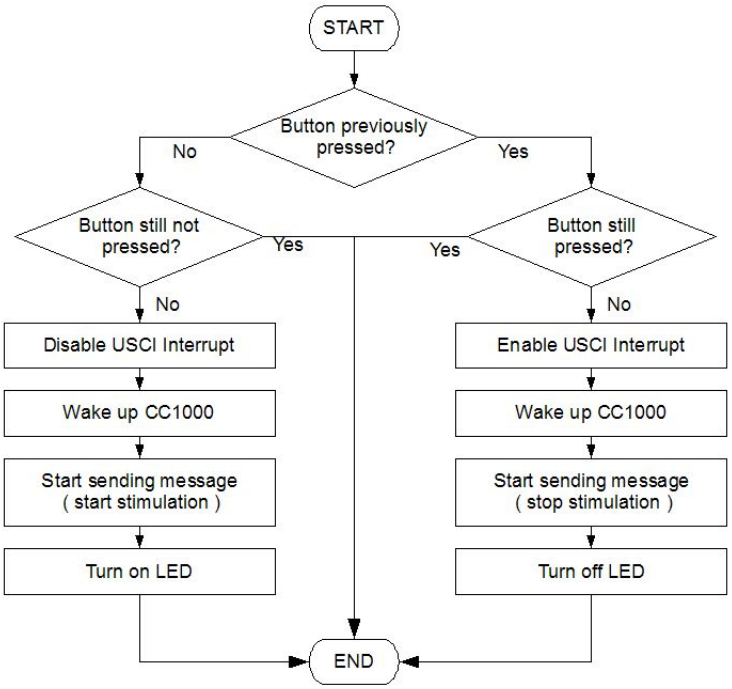

Figure 25: Timer_A0 ISR for button polling

Universal Serial Communication Interface and communication with the PC

The Universal Serial Communication Interface (USCI) can be configured to work similarly like the common Universal Asynchronous Receiver/Transmitter (UART) in embedded systems; it can handle communication with the RS232 port of the PC. Data are sent serially in frames, each of which contains one byte of payload, one low level Start bit, and one high level Stop bit (8N1 format, no parity bit). The Baud rate was set to 9600 Bauds. Contrary to the CC1000 wireless chip, the USCI can receive and transmit frames of data independently by hardware, software only has to read the appropriate registers when the USCI interrupt triggers. The flowchart of the interrupt handler can be seen in Figure 26.

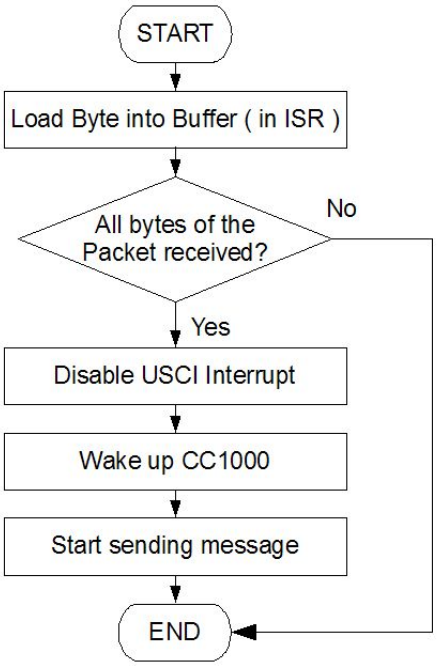

Figure 26: The USCI interrupt routine in main loop

6 Performance analysis

Current consumption

Almost all design steps focused on the reduction of current consumption of the boards. It is crucial to assess, how well this goal was accomplished. The following section will provide theoretical current profiles of the two designed PCBs, which will be followed by concrete measurements.

Stimulator board

A failed attempt by the CC1000 to find valid preamble lasts approximately 2 ms. With the polling period of 50 ms we can conclude, that the chip spends about 96% of its lifetime in low power mode. If a valid packet is detected, it takes maximum 95 ms to receive it (912 bits at 9600 bit/s). Using Table 2 and the assumption, that there is very little wireless traffic, the expected power consumption of the CC1000 on the stimulator board can be estimated by:

$$I_{avg,CC1000rec} \approx 0.04 * 7.4mA + 0.96 * 200nA \approx 0.3\text{mA}$$

The MSP430 microcontroller spends about 90% of the time in low power mode 'LPM0' , where the CPU and its clock is disabled. The MSP430 is capable to shut down its DCO to conserve even more power, but this feature could not be used as some peripherals always required the DCO as clock source. Using [17] the current consumption of the microcontroller is:

$$I_{avg,MSP430stim} \approx 0.2 * 2.4 + 0.8 * 0.56 \approx 0.93\text{mA}$$

The LED (forward voltage drop=0.6V) is operated with a 510 Ohm resistor with 50% duty cycle, which gives us

$$I_{avg,LED} \approx \frac{1}{2}\frac{(3-0.6)}{510} \approx 2.3\text{mA}$$

The estimated current consumption of the stimulator output stage is very difficult to determine, as it was discussed in section 3.2. An estimation using equation 32 for $f_s = 5.7$kHz, D=20%, $U_o = 200V$ is: $I_{avg,boost} \approx 1.6$mA.

This results in the total current consumption of the stimulator board, as 5.13 mA while stimulation is in progress, and 1.23 mA otherwise. The actual measured values were fairly close; 6.4 mA during stimulation and 1.3 mA in 'standby'.

The rated capacity of the 2320 battery is 220 mAh, which leaves35 hours of estimated battery life with and 169 hours without stimulation. The stimulated lifetime of the device could be extended to 53 hours just by simply removing the LED. Practically these figures could be misleading, as actual battery capacity strongly depends on the mean value and distribution of current discharge[26]. Figure 7 on the other hand shows that the current drawn from the battery is very uneven, which might shorten battery life. Nevertheless it can be concluded that the estimated lifetime of the designed stimulator is highly superior to the RehaStim stimulator, which can only run for 6 hours from a 6 V battery.

Interface board

The theoretical power consumption of the interface board was calculated similarly, as can be seen in Table 7. The CC1000 chip only wakes up if data are waiting to be sent. This is assumed to be very infrequent, thus power down mode current consumption profile was adapted.

	current consumption
MSP430	~1 mA
CC1000	~0.2 μA (in PD mode)
MAX3232	1 mA
LED (50% duty cycle)	2.3 mA

Table 7: Estimated power consumption of the stimulator

This time the measured current consumption was unexpectedly high, 7.6 mA while stimulating with the button (LED flashes), and 6.3 mA otherwise. Even this gives about 400 hours of lifetime using typical AA batteries.

Stimulation

The stimulator's stimulation capabilities were tested with a load of 1 kOhm. As it was discussed in section 2.4, this is a typical value for well prepared skin surfaces.

The current amplitude was tested in the range of 5-100 mA. The accuracy of the output current was found to be dependent on other stimulation parameters, but generally higher current values could be more precisely set by the digital controller. This is probably due to the fact that the microcontroller has no floating point unit and it handles fractions with difficulty (expressed in high computational power), therefore all calculation results were rounded to the nearest integers. The accumulated error was more explicit while handling lower numbers (this phenomenon affects the accuracy of all stimulation parameters). It must also be mentioned, that depending on pulse width the maximal current value of the decaying pulse top was sometimes multiple of the desired average level. This is due to the fact that the digital controller samples the feedback in the middle of the pulse. This approach provides more precise control of the injected charge, than sampling the maximal current value, but it cannot have control over the maximal current flowing through the body. This is one of the serious limitations of this design compared to professional commercial solutions. The stimulator was found capable of outputting current levels in the tested range, while the pulse repetition frequency was 50 Hz and the pulse width was set to 100 μs (see Figures 27b and 27a).

	wireless stimulator*		RehaStim	
	minimum	maximum	minimum	maximum
Current amplitude	0	100 mA	0	126 mA
Pulse waveform	monophasic or biphasic		any	
Pulse repetition frequency	25 Hz	300 Hz	1 Hz	140 Hz
Pulse width	$40\mu s$	$500\mu s$	$20\mu s$	$500\mu s$
rise time of pulse		1 μs		2 μs
number of channels	1		8	
wireless connectivity	available		not available	
Battery life	35 hours from 2 AA batteries		9 hours from 4 AA batteries	
Size	5.7 x 4.3 x 2 cm		15.5 x 6.5 x 13.5 cm	

Table 8: Characteristics of the wireless stimulator in comparison with the specified technical details of RehaStim[2].
*The measurement conditions can be found in the text.

The pulse duration was tested with the current amplitude of 20 mA and pulse repetition frequency of 50 Hz. The output stage was found capable of producing pulses in the 40-500 μs range, although by measuring PW=500 μs the output capacitor discharged totally (the voltage dropped to 0) by the end of the pulse. This suggests that the entire pulse width spectrum cannot be utilised under all conditions (low current amplitude, etc). The narrowest pulse width is also below the capability of RehaStim.

The frequency range of the stimulator was found most deficient. The boost converter of the output stage didn't tolerate pulse repetition frequencies lower than 10 Hz, and the accuracy of pulse amplitudes were found unacceptable with frequencies under 25 Hz (see Figure 27c). The conditions of this measurement were I=20 mA, PW= 200 μs. The maximal adjustable frequency with accurate current amplitude was 300 Hz (see Figure 27d).

The rise time of the stimulator was also measured, and it was found to be competitive with RehaStim (200 ns at PW=200 μs, I=20 mA, f=50Hz).

I also carried out measurements with a higher, 5 kOhm load resistor, which intends to model unprepared skin impedances. With the increased load the pulse tops became flatter (larger RC time constant), but the simulator couldn't output currents higher than 35 mA (see Figure 27f). This is the point where the inductor in the boost converter saturates and increasing the boost converter's duty cycle results in no further output voltage level gain. Higher current outputs could be achieved by fine tuning the inductor used in the stimulator circuit (see section 3.2). For the parameter overview of the designed stimulator device, and a comparison with RehaStim, please refer to Table 8.

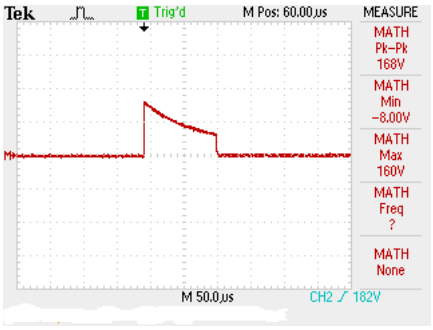

(a) High current monophasic pulses, $R_{load} = 1kOhm$, I=100 mA, f=50Hz, $PW = 100\mu s$

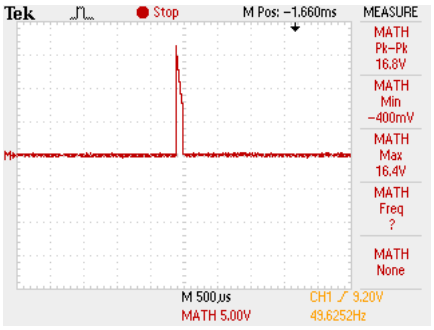

(b) Low current monophasic pulses, $R_{load} = 1kOhm$, I=5 mA, f=50Hz, $PW = 100\mu s$

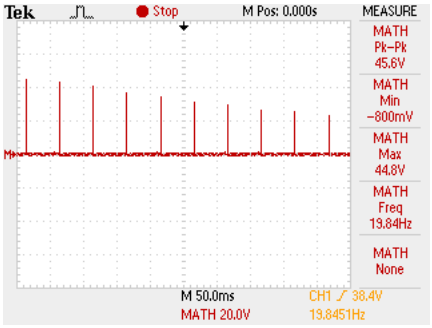

(c) Low frequency monophasic pulses, $R_{load} = 1kOhm$, I=20 mA, f=20Hz, $PW = 200\mu s$

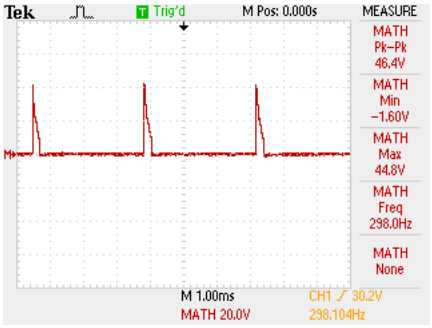

(d) High frequency monophasic pulses, $R_{load} = 1kOhm$, I=20 mA, f=300Hz, $PW = 200\mu s$

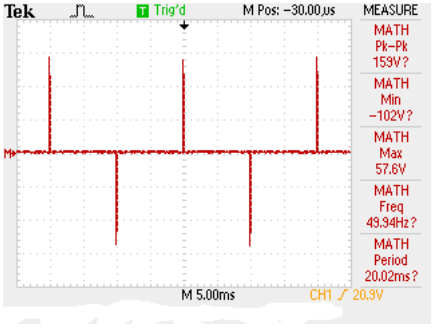

(e) Biphasic pulses, $R_{load} = 5kOhm$, I=20 mA, of 10 mA, f=50Hz, $PW_{pos} = PW_{neg} = 100\mu s$

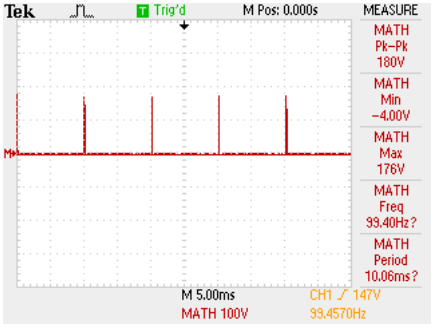

(f) High load high voltage monophasic pulses, $R_{load} = 5kOhm$, I=35 mA, f=100 Hz, $PW_{pos} = 100\mu s$

Figure 27: Oscilloscope measurements of stimulator output pulses

Working range

The device could be safely controlled from distances up to 15 m (although only limited tests were made). Moving away any further might result in packet loss and the unreliable control of stimulation. The working range could be easily extended by request, if the output power of the CC1000 would be set to 10 dBm. It must also be noted that the measurement was carried out indoors, where the device will most likely be operated. Possibly a better performance could be achieved outdoors due to mitigation of multipath fading[25].

Board size

The dimensions of the stimulator PCB are 5.7 x 4.3 x 2 cm. It should fit comfortably on the stimulation body surfaces of interest. For multichannel stimulation of various muscle groups at the same time, several stimulator boards could be used. Section 8 will provide more details about this idea.

Patient safety

The stimulator is absolutely safe and can cause no harm to patients. The worst case scenario is when the output capacitor is touched while it is charged to 300 V, which drives 30 μC (Q=CU) of charge though the human body. This is well below the dangerous limit of 560 μC, as calculated by [27].

7 User's guide

While reading the following guide please refer to Figure 28 showing images of the designed PCBs.

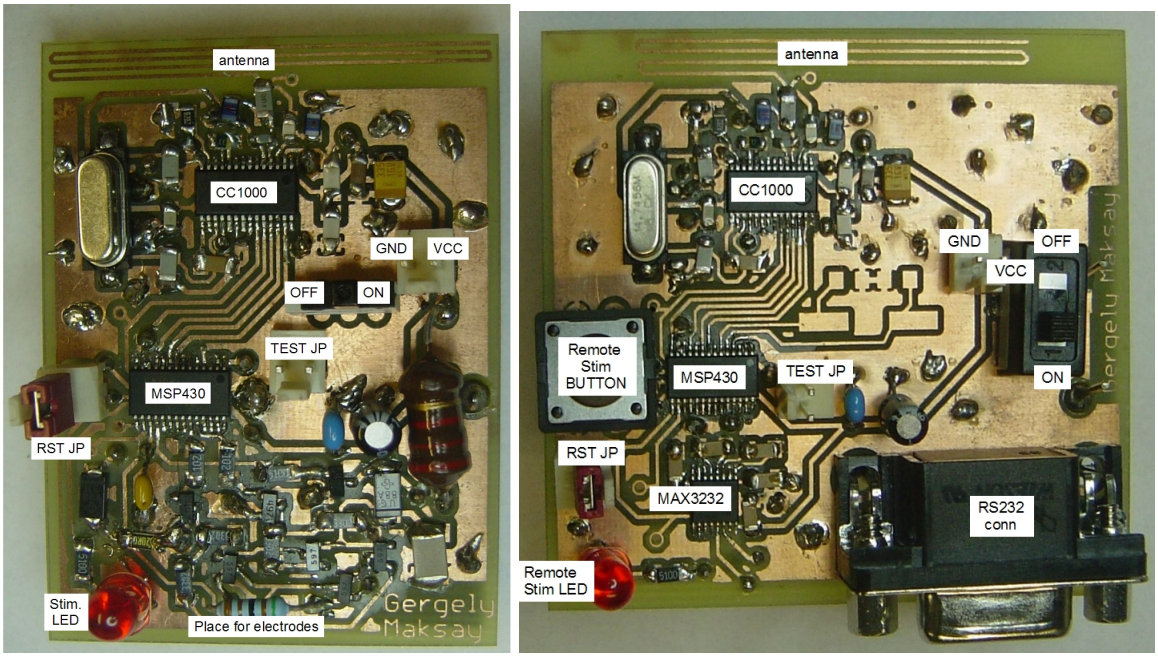

(a) Stimulator board (b) RS232/Wireless interface board

Figure 28: Front view image of the boards

The following steps are required to set up the stimulator board for neuromuscular stimulation:

1. Connect the interface board's 9 way D-type connector (standard RS232 connector) to the RS232 serial port of the laptop or personal computer (alternatively an USB-serial converter can be used)

2. Put the stimulator module's electrodes to the skin surface, where the muscles to be stimulated are located. Note, that the stimulator is still in testing stage, at present a 5 kOhm resistor is placed where the electrodes should be connected.

3. On the PC/laptop open Matlab and run Stimulator.m. The graphical user interface (GUI) displayed in Figure 29 will pop up.

4. Set the serial port number in Matlab (it can be checked in Control Panel/System/Hardware/Device Manager under Windows, or using the 'setserial' command under Linux).

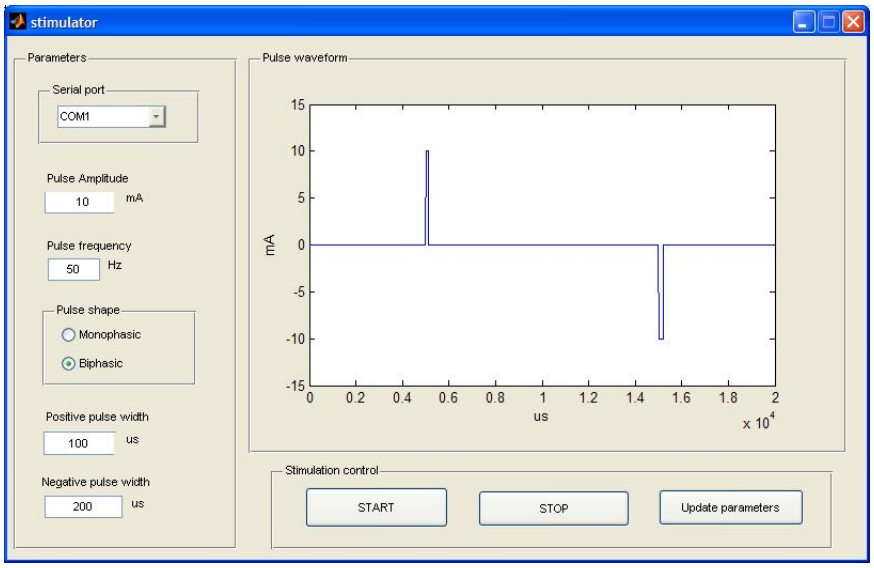

Figure 29: Matlab program's graphical user interface

5. Make sure that the red JUMPER RST JP is placed on both the stimulator board and the interface board.

6. Turn on the stimulator module and the interface board. Look for a short blink of the LED indicating that the board is ready for stimulation.

7. Set the required stimulation parameters on the left side of the MATLAB GUI. The graph on the right side of the screen will provide a visual representation of the resulting pulse waveform. Note, that pulse frequency is interpreted as the frequency of pulses with same polarity, even if biphasic stimulation is selected. The program is protected against entering meaningless or invalid input values.

8. Press the Update button to transfer the parameters into the stimulation board.

9. Press the START button to activate stimulation. It can be stopped any time with the STOP button. The stimulator parameters can be set runtime as well, the stimulation will continue uninterrupted with the updated parameters. The 'Stim LED' on the stimulator board always flashes as long as stimulation is in progress.

If the stimulation is started before the parameters were programmed, the following default values will be assumed:

- Pulse amplitude = 10 mA
- Pulse frequency = 50 Hz

- Pulse shape = biphasic
- Positive pulse width = $100\mu s$
- Negative pulse width = $100\mu s$

If a PC with an RS232 port is not available, the stimulator can be directly started and stopped with the button on the interface board, like a remote controller. Stimulation will occur while the button is pressed down with default parameters. The 'Remote Stim LED' on the interface board will start flashing, to indicate that remote controlled stimulation is in progress.

Developer's guide

Please refer to my notes about the development environment and development tools in section 5.1. Connect the FET tool to the USB port of your PC, and to the 14 pin JTAG connector on your programming interface board (find it in the appendix). Remove RST JP from both boards, and connect the RST, TEST, GND and VCC pins with the corresponding pins on the programming interface board (watch out for the right pins on RST JP, shown in Figure 28 with labeling). The programming of the board can already be initiated.

8 Future development plans

One of the greatest shortcomings of the designed stimulation system is that it is not capable to produce a multichannel output, which is utterly needed in FES. Multiplexing the stimulation output is a possible workaround in future versions of the design, however the small size of the stimulator board enables the application of several boards on the intended muscles. This solution requires minor modifications in software. The communication protocol (Table 3) must be extended with a field that identifies the address of the stimulator, and allows independent control for all stimulator boards in use. The addresses can be static with the modification of the embedded software in each stimulator device, or they can be dynamically distributed from the PC. The latter solution would require the implementation of half duplex communication, which could be easily done based of the currently running code.

The implementation of half duplex communication can offer further advantages in future versions. A more reliable wireless communication could be established by handshaking, the stimulator could send an acknowledge packet to notify the PC of the successful reception of a packet. The packet could also contain an 8 bit checksum or CRC (cyclic redundancy check), which could verify the data integrity. If needed, request for retransmission could be sent to the PC.

In the current design, monophasic, or biphasic pulses can be produced with given frequency, pulse width and current amplitude. The flexibility of the pulse waveforms could be greatly enhanced, if the PWM determining the pulse widths would be generated by the ISR of the Timer in continuous mode. Although this requires additional processing and thus increased current consumption, bursts of pulses could be produced with entirely arbitrary waveform (only current amplitude would be fixed). A buffer could contain the parameters of the pulses in blocks of 2 bytes, one byte determining the pulse width, and the next byte the space until the next pulse. One bit of either of these bytes could be reserved to determine the phase of the pulse. The Timer could circularly read this buffer and repeatedly measure the time until the next pulse transition. This would also mean a reduction in accuracy compared to the hardware driven solution, but it offers endless flexibility.

Although not directly related to FES, muscle training often requires 'modulation mode' stimulation where the pulse amplitude is gradually increased[3] for elevating muscle stress. This could be also implemented with the above described modification, although the digital controller needs certain number of pulses to set the desired current amplitude, which limits the rate of current amplitude rise.

Apart from the channel multiplexing, all suggestions so far could be easily implemented by sole software amendments with little effort. The following suggestions require extension of hardware which results in size and current consumption increase. It must be carefully evaluated if it is worth this compromise.

The current design includes no voltage regulator, which might result in the unpredictable operation of the device with sinking battery voltage. A DC-DC

converter IC could be adapted for this task. As an alternative solution the MSP430 microcontroller's analog-digital converter is capable of measuring the supply voltage, and a low battery indicator LED could notify the user if needed.

The capabilities of the CC1000 chip are far beyound the current implementation of the device. It could be further exploited for various research projects. For instance biosignals (EMG, EEG, ENG) could be acquired and transmitted to the PC wirelessly, which could be processed as feedback to closed loop controlled neuroprostheses. This is one of the emerging technologies, which might promise a breakthrough in the rehabilitation of paraplegics[5].

9 Conclusion

A transcutaneous neuromuscular stimulation system has been designed and implemented. The stimulator device can generate high voltage constant current regulated faradic stimulation pulses with flexibly adjustable current amplitude (0-100 mA), pulse width (40-500 μs) and pulse repetition frequency (25- 300 Hz). These parameters can be configured remotely from a personal computer over a wireless link. The entire system is operational, including the stimulator board responsible for generating the high voltage pulses, an interface board which directs the commands from the PC to the stimulator over a radio frequency link, and the Matlab software which interacts with the operator through a graphical user interface.

Even though the quality of produced waveform is inferior to professional commercial solutions, like RehaStim (decaying pulse top, only one channel, less flexible pulse waveform, etc.), the wireless connectivity, cheaper cost, smaller size, lighter weight, and prolonged lifetime from battery make the presented stimulation system a competitive product in numerous applications. Although it was specially designed for functional electrical stimulation, its capabilities make it universally deployable in therapy, as well as research.

Appendix

Schematic of stimulator board

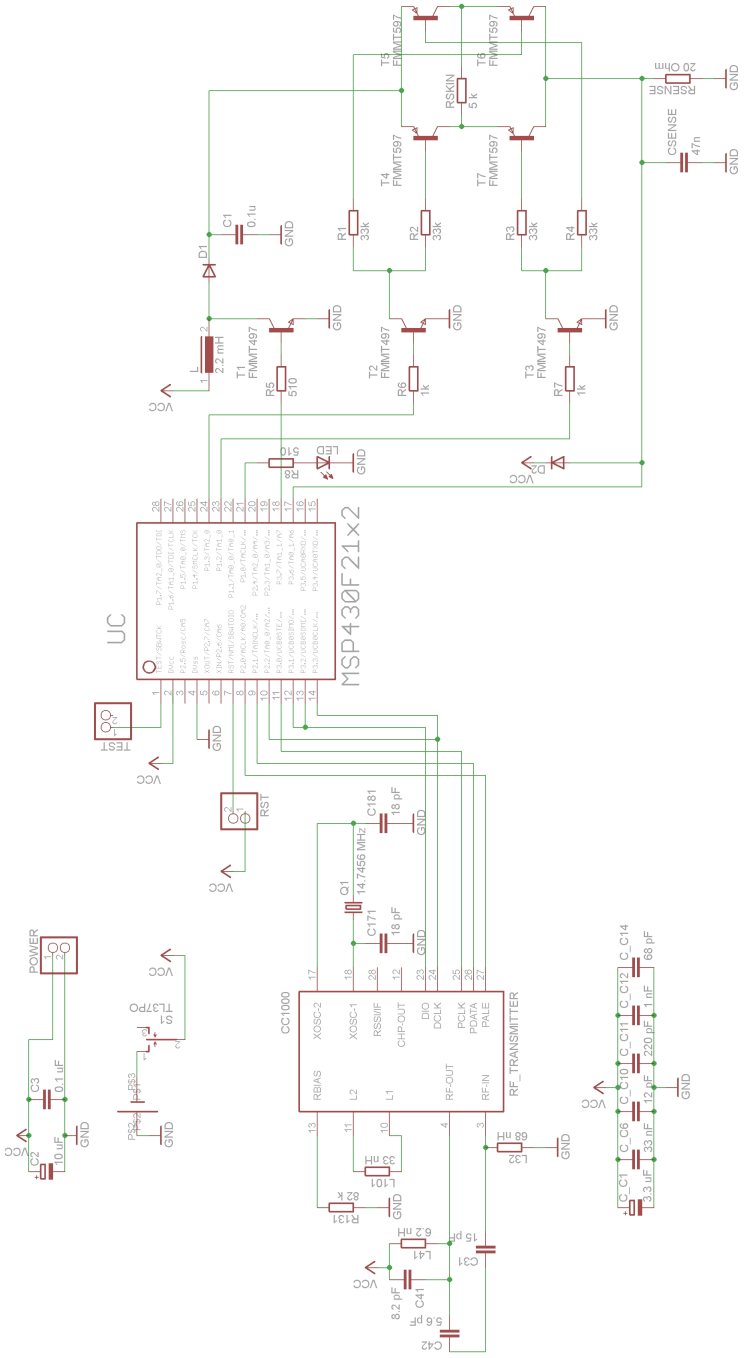

Layout of stimulator

Top:

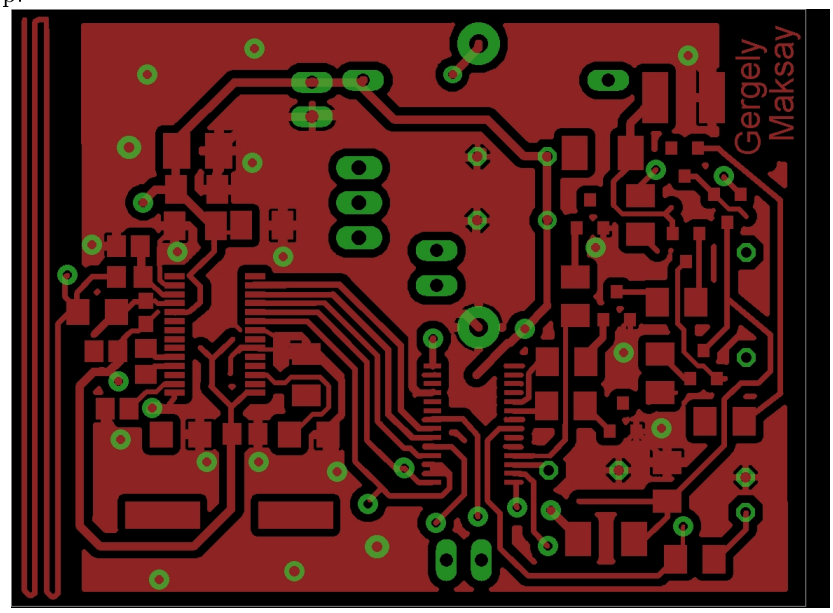

Bottom:

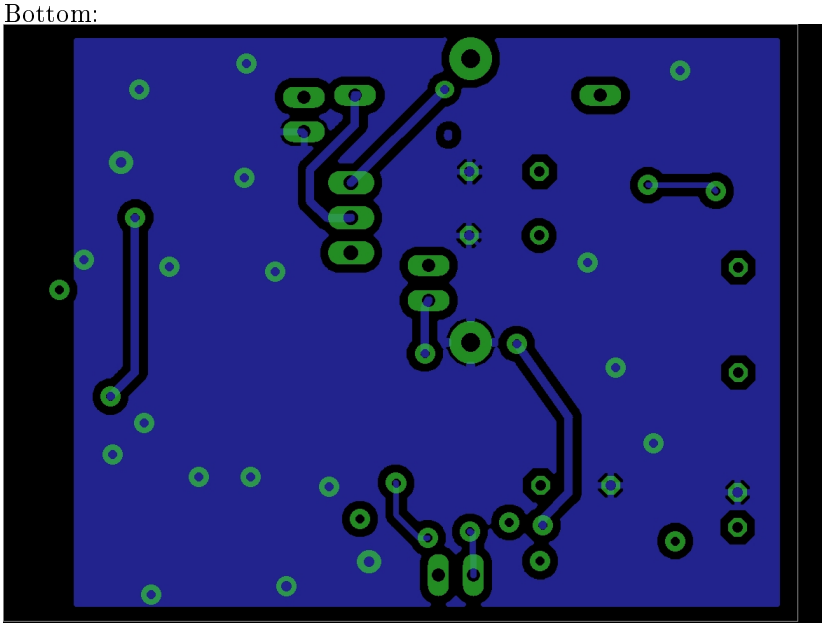

Stimulator Bill of Materials

reference	description	value
C1	400 V SMD capacitor	0.1 μF
C2	electrolytic capacitor	10 μF
C3	ceramic capacitor	0.1 μF
C_C1	SMD tantalum capacitor	3.3 μF
C_C6	SMD ceramic capacitor	33 nF
C_C10	SMD ceramic capacitor	12 pF
C_C11	SMD ceramic capacitor	220 pF
C_C12	SMD ceramic capacitor	1 nF
C_C14	SMD ceramic capacitor	68 pF
C171	SMD ceramic capacitor	18 pF
C181	SMD ceramic capacitor	18 pF
C41	SMD ceramic capacitor	8.2 pF
C42	SMD ceramic capacitor	5.6 pF
C31	SMD ceramic capacitor	15 pF
L	inductor, 220 mA	2.2 mH
L41	SMD inductor	6.2 nH
L101	SMD inductor, high Q	33 nH
L32	SMD inductor	68 nH
T1	npn transistor	
T2	npn transistor	
T3	npn transistor	
T4	pnp transistor	
T5	pnp transistor	
T6	pnp transistor	
T7	pnp transistor	
Csense	ceramic capacitor	47 nF
Q1	SMD crystal	14.7456 MHz
R131	SMD resistor	82 kOhm
R1	SMD resistor	33 kOhm
R2	SMD resistor	33 kOhm
R3	SMD resistor	33 kOhm
R4	SMD resistor	33 kOhm
R5	SMD resistor	510 Ohm
R6	SMD resistor	1 kOhm
R7	SMD resistor	1 kOhm
R8	SMD resistor	510 Ohm
Rsense	SMD resistor, 0.1%	20 Ohm
LED1	LED, red	
D1	SMD diode, 1A	
D2	SMD diode, 1A	
uC	MSP430F2122	
CC1000	CC1000	

Wireless/RS232 Interface board schematic

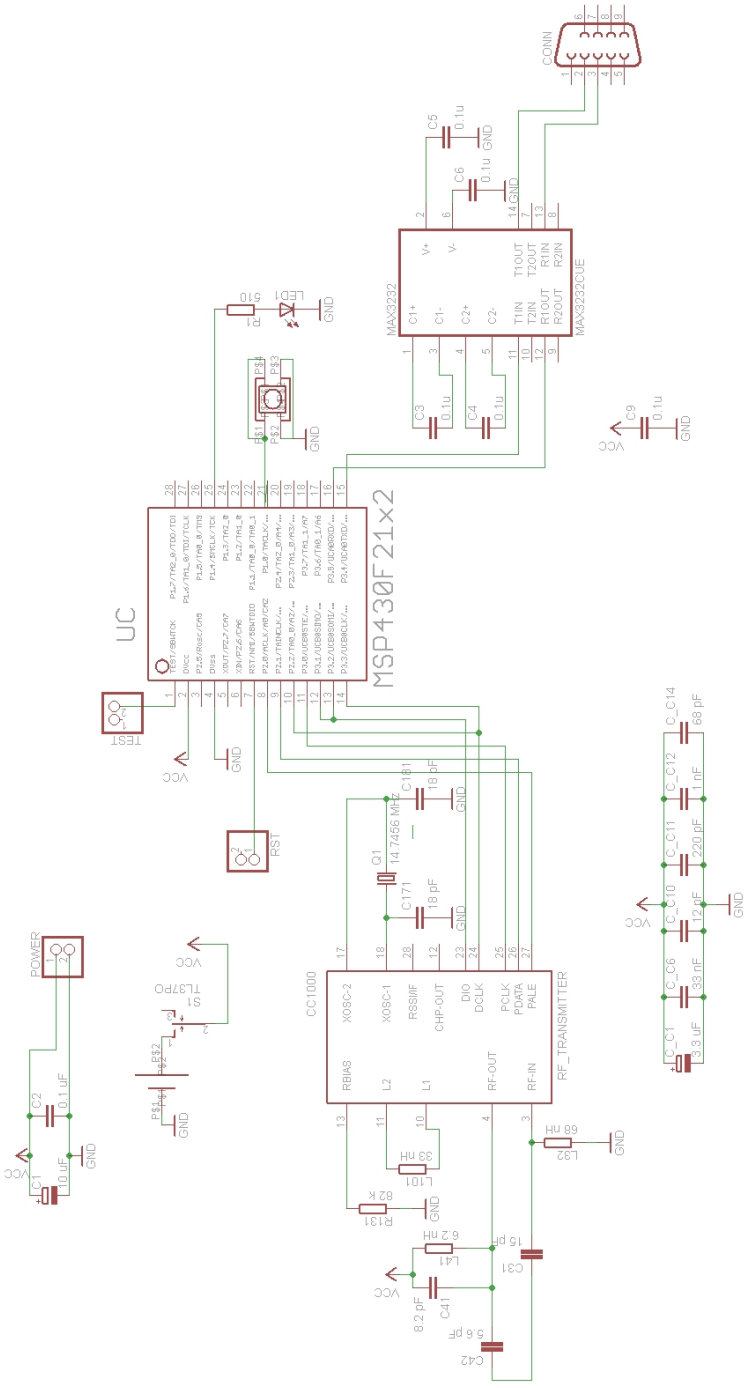

Layout of Wireless/RS232 Interface board

Top

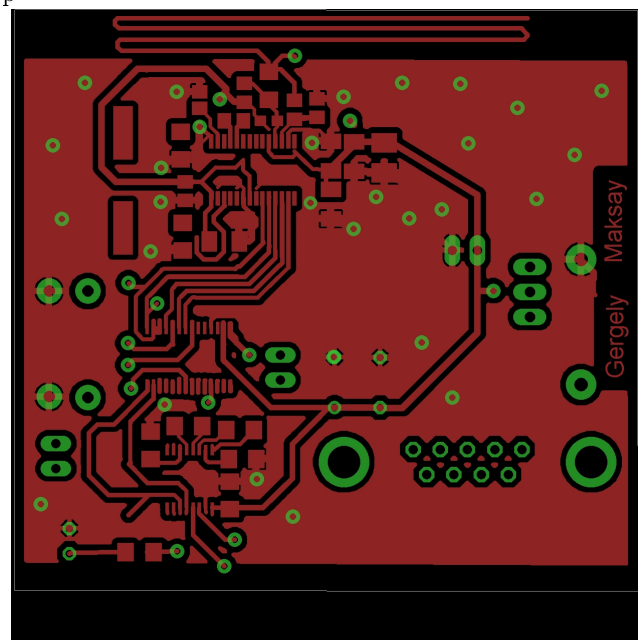

Bottom:

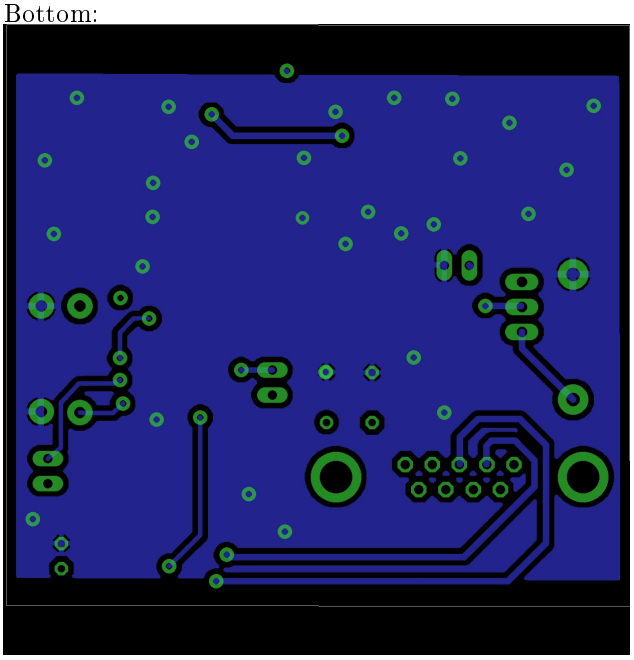

Wireless/RS323 Interface Board, Bill of Materials

reference	description	value
C1	electrolytic capacitor	10 μF
C2	ceramic capacitor	0.1 μF
C3	SMD ceramic capacitor	0.1 μF
C4	SMD ceramic capacitor	0.1 μF
C5	SMD ceramic capacitor	0.1 μF
C6	SMD ceramic capacitor	0.1 μF
C9	SMD ceramic capacitor	0.1 μF
C_C1	SMD tantalite capacitor	3.3 μF
C_C6	SMD ceramic capacitor	33 nF
C_C10	SMD ceramic capacitor	12 pF
C_C11	SMD ceramic capacitor	220 pF
C_C12	SMD ceramic capacitor	1 nF
C_C14	SMD ceramic capacitor	68 pF
C171	SMD ceramic capacitor	18 pF
C181	SMD ceramic capacitor	18 pF
C41	SMD ceramic capacitor	8.2 pF
C42	SMD ceramic capacitor	5.6 pF
C31	SMD ceramic capacitor	15 pF
L41	SMD inductor	6.2 nH
L101	SMD inductor, high Q	33 nH
L32	SMD inductor	68 nH
Q1	SMD crystal	14.7456 MHz
R131	SMD resistor	82 kOhm
R8	SMD resistor	510 Ohm
LED1	LED, red	
CONN	9-way D-type connector	
MAX3232	MAX3232 CUE	
uC	MSP430F2122	
CC1000	CC1000	

JTAG programming interface board, schematic

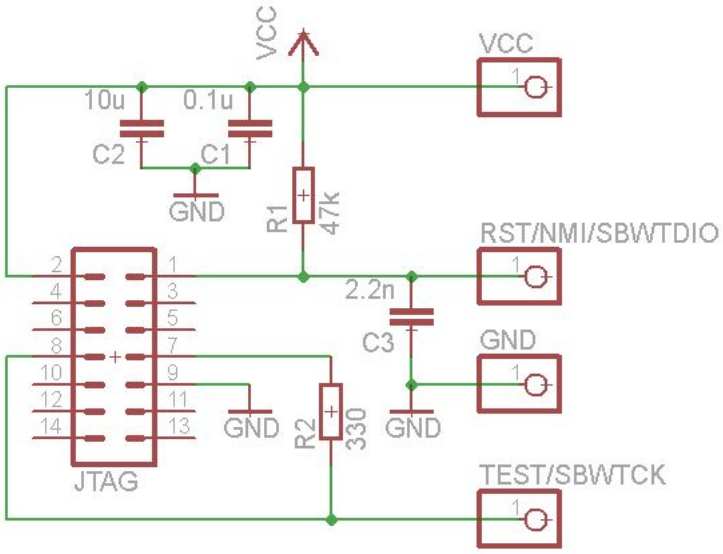

References

[1] Centre for Rehabilitation Engineering, Glasgow University, `http://www.gla.ac.uk/cre/`

[2] Hasomed GmbH, `http://www.hasomed.de`

[3] Sheila Kitchen, *"Electrotherapy : Evidence based practice, Eleventh Edition"*, Churchill Livingstone, 2002

[4] Jaakko Malmivuo, Robert Plonsey, *"Bioelectromagnetism - Principles and Applications of Bioelectric and Biomagnetic Fields"*, Oxford University Press, New York, 1995.

[5] P. Hunter Peckham, Jayme S. Knutson, *"Functional electrical stimulation for Neuromuscular applications"*, Annual Review of Biomedical Engineering, pp. 327-360, 2005

[6] Jay T. Rubinstein, Charles A. Miller, Hiroyuki Mino, Paul J. Abbas, *"Analysis of Monophasic and Biphasic Electrical Stimulation of Nerve",* IEEE Transactions on biomedical engineering, vol 48, pp. 1065-1070, 2001

[7] A. van Boxtel, *"Skin resistance during square wave electrical pulses of 1 to 10 mA"*, Med and Biol. Eng & Comput, volt 15, pp. 679-687, 1977,

[8] J. Patrick Reilly, *"Applied Bioelectricity: From Electrical Stimulation to Electropathology"*, Springer, 1998

[9] Stephen J. Dorgan, Richard B. Reilly and Carl D. Murray, *"A model for human skin impedance during surface functional neuromuscular stimulation"*, Proceedings - 19th International Conference - IEEE/EMBS, pp. 1770-1773, 1997

[10] T Ragheb, L A Geddes, *"Electrical properties of metallic electrodes"*, Medical and Biological Engineering and Computing, pp. 182-186, 1990

[11] Perkins TA, *"Impedances of common surface stimulation electrodes"*, 9th Annual Conference of the International FES Society, 2004

[12] H.W. Whittington, B. W.Flynn, D.E. Macpherson, *"Switched mode power Supplies : Design and construction"*, Research Studies Press Ltd., 1992

[13] Robert W. Ericsson, Dragan Maksimovic, *"Fundamentals of Power Electronics, Second Edition"*, Kluwer Academic Publishers, 2004

[14] International Telecommunication Union website, `http://www.itu.int/ITU-R/terrestrial/faq/index.html`

[15] Ferrel G. Stremler, *"Introduction to Communication Systems, Third Edition"*, Addison-Wesley Publishing Company, 1997

[16] Matthew Loy, Iboun Sylla, Texas Instruments Inc., *"Application Report SWRA046A, ISM-Band and Short Range Device Antennas"*, 2005

[17] Texas Instruments Inc., *"MSP430F21x2 Mixed Signal Microcontroller, SLAS578D"*, 2009

[18] Texas Instruments Inc., *"MSP430x2xx Family User's Guide, SLAU144E"*, 2008

[19] John Davies, *"MSP430 Microcontroller Basics"*, Elsevier Ltd., 2008

[20] MSPGCC, The GCC toolchain for the Texas Instruments MSP430 MCUs, `http://mspgcc.sourceforge.net`

[21] Texas Instruments Inc., *"CC1000 Single Chip Very Low Power RF Transceiver, SWRS048A"*, 2009

[22] K. H. Torvmark, Texas Instruments Inc., *"AN009 CC1000/CC1050 Microcontroller interfacing, SWRA082"*

[23] Texas Instruments Inc.," User Manual, Rev. 1.22, CC1000PP Plug and Play Module, SWRU060"

[24] Keith Quiring, Texas Instruments Inc., *"Application Report SLAA294A, MSP430 Software Coding Techniques"*, 2006

[25] K. H. Torvmark, Texas Instruments Inc., *"Application Note AN015 SWRA076 RF Modem Reference Design"*

[26] Massoud Pedram, Qing Wu, *"Design considerations for battery-powered electronics"*, Design Automation Conference, pp.861 - 866 , 1999

[27] Kurt A. Kaczmarek, Kevin M. Kramer, John G. Webster, Robert G. Radwin, *"A 16-Channel 8-Parameter Waveform Electrotactile Stimulation System"*, IEEE Transactions on Biomedical Engineering, 1991